Weather and Climate Extremes 39 (2023) 100542

Contents lists available at ScienceDirect

Weather and Climate Extremes

journal homepage: www.elsevier.com/locate/wace

The influence of an atmospheric river on a heavy precipitation event over the western Alps

Silvio Davolio [a,*], Marco Vercellino [b], Mario Marcello Miglietta [c], Lucia Drago Pitura [a,b], Sante Laviola [a], Vincenzo Levizzani [a]

[a] Institute of Atmospheric Sciences and Climate, National Research Council, CNR-ISAC, Bologna, Italy
[b] Formerly Department of Physics and Astronomy, University of Bologna, Bologna, Italy
[c] Institute of Atmospheric Sciences and Climate, National Research Council, CNR-ISAC, Padua, Italy

ARTICLE INFO

Keywords:
Heavy precipitation
Atmospheric river
Mediterranean
Moisture transport
Orographic precipitation

ABSTRACT

On 2–3 October 2020, a heavy precipitation event severely affected northern Italy and in particular the western Alps, with rainfall amount exceeding 600 mm over 24 h. This event was associated with an upper-level trough over the western Mediterranean basin, a large-scale configuration typical of heavy precipitation phenomena on the southern side of the Alps, since it induces a northward transport of large amounts of moisture impinging on the orography. The present study shows that a relevant amount of moisture moved towards the Mediterranean basin in the form of an atmospheric river (AR), a long and narrow filament-shaped structure crossing the whole Atlantic Ocean, characterized in the present case by a maximum Integrated Vapour Transport exceeding 1000 kg m^{-1} s^{-1}. Therefore, in addition to the local contribution from the Mediterranean Sea, a relevant amount of moisture moved from the Tropics towards the Mediterranean, feeding the precipitation systems.

The presence of an AR represented a distinguishing aspect of the event, superimposed on the well-known dynamic-thermodynamic mechanisms of heavy precipitation over the Alps. High-resolution numerical simulations and diagnostic tools have been exploited to investigate in detail how the transport of water vapour associated with the AR has influenced the dynamics and favoured the severity of the heavy precipitation processes.

The results disclose the role of the AR and add further details to the theoretical framework of heavy precipitation mechanisms in the Alpine area, improving our understanding of the complex interaction between large-scale flows and mesoscale dynamics during extreme precipitation episodes. Due to the relatively fast evolution of the synoptic disturbance, the typical mesoscale mechanisms would have led only to an ordinary intense rainfall event. The contribution of the AR turned the event into a devastating flood.

1. Introduction

Heavy precipitation in the Mediterranean area, and especially over the Alps, has been and is still a topic of vivid interest within the scientific community, given the destructive floods that every year produce severe impacts and threat to the population (Isotta et al., 2014; Dayan et al., 2015; Khodayar et al., 2021). Research efforts have focused on a better understanding of the mechanisms responsible for extreme rainfall as a step necessary to improve forecasting. Since the Mesoscale Alpine Programme field campaign in 1999 (MAP, Bougeault et al., 2001), several efforts have been devoted to identify the linkage between large scale conditions and heavy precipitation over the Alps (Rotunno and Houze, 2007, among others). In these events, the presence of a large amplitude wave, i.e. a pronounced upper level Potential Vorticity anomaly (Massacand et al., 1998), slowly evolving eastward over the western Mediterranean, is a common feature that has been recently connected to pronounced undulations in the upper-tropospheric jet and Rossby wave packets (Grazzini et al., 2021). Grazzini et al. (2020a) identified, in all three different categories of synoptic patterns associated with extreme rainfall over northern Italy, the presence of a trough over western Europe and the Mediterranean, although slightly different in position and intensity. On the other hand, recent outcomes of the HyMeX Programme and its field campaign (Drobinski et al., 2014; Ducrocq et al., 2014) have highlighted some important physical processes and features at the mesoscale that are often associated with heavy precipitation and convection on the whole basin (Khodayar et al., 2021), and specifically

* Corresponding author. CNR- ISAC, Via Gobetti 101, Bologna, 40129, Italy.
E-mail address: s.davolio@isac.cnr.it (S. Davolio).

https://doi.org/10.1016/j.wace.2022.100542
Received 19 July 2022; Received in revised form 9 December 2022; Accepted 15 December 2022
Available online 19 December 2022

on the Italian peninsula (Miglietta and Davolio, 2022).

In association with the dynamical forcing, moisture availability is another key ingredient for heavy precipitation in the Mediterranean (Khodayar et al., 2018; Grazzini et al., 2020a; de Vries, 2021). In fact, several recent studies analysed the role of anomalous integrated water vapour transport towards the region. Just to mention a few, Sodemann and Zubler (2010) showed that, even within a relevant case-to-case variability, the Mediterranean is clearly not the only source of humidity in the region. Winschall et al. (2012, 2014) identified different sectors of the Atlantic Ocean feeding precipitation events well downstream, even over the Alps. The role of the Atlantic was also pointed out by Pinto et al. (2013). Additionally, relevant amounts of moisture can travel towards the Mediterranean basin from the Tropics, when an upper-level trough develops deeply into North Africa (Turato et al., 2004; Krichak et al., 2015; Chazette et al., 2016). A recent study (de Vries, 2021) pointed out that extreme precipitation events in the midlatitude are often modulated by the combined occurrence of Rossby wave breaking and intense moisture transport. The strong upper tropospheric forcing favours poleward moisture injections and also rising motion by reducing the atmosphere static stability.

In spite of the large number of studies focusing on extreme precipitation on the Alps, only in the last years it has been recognised that the moisture transport towards and over the Mediterranean may assume the form of an atmospheric river (AR; Ralph et al., 2018). In fact, previous studies only suggested the link between rainfall over Italy and tropical moisture transport (Bertò et al., 2004; Malguzzi et al., 2006; Buzzi et al., 2014), but only Krichak et al. (2015) analysed the Integrated Vapour Transport (IVT) field to assess the presence of an organized moisture transport, although without applying an objective identification algorithm. More recently, Davolio et al. (2020a) revealed the presence and the role of an AR associated with a very intense Mediterranean storm occurred in October 2018 (Cavaleri et al., 2019; Giovannini et al., 2021). Finally, ARs over the Mediterranean affecting both the Iberian Peninsula (Lorente-Plazas et al., 2019) and the eastern basin (Bozkurt et al., 2019) were analysed, showing that besides heavy precipitation, ARs may be associated with other severe environmental phenomena such as snow melting and dust transport (Francis et al., 2022).

At the mesoscale, vapour transport towards the Alps is often organized in the form of a pre-frontal meridional low-level jet over the Tyrrhenian Sea (e.g., Buzzi and Foschini, 2000), in response to a trough over the western Mediterranean (relevant geographical details in Fig. 1). The thermodynamic characteristics of the impinging moist flow are fundamental to determine the interaction with the orography (Miglietta and Rotunno, 2014) and thus the space/time distribution of the rainfall. In particular, from the analysis of one infamous flooding episode affecting the Piedmont region in 1994 (described in Grazzini et al., 2020b; Davolio et al., 2020b) and other successive severe events, Rotunno and Ferretti (2001, 2003) provided an enlightening picture of the mesoscale mechanisms responsible for heavy precipitation over the western Alps. The orographic uplift of the pre-frontal southerly moisture-laden flow is enhanced due to the convergence with an easterly low-level current over the Po valley, coming from the Adriatic basin (see Fig. 8e in Rotunno and Ferretti, 2003). The latter flow is more stable, thus it is deflected in front of the Alps as a barrier wind (Buzzi et al., 2020) and undercuts the main southerly stream, before they rise together over the Alpine chain. The persistence of this pattern, favoured by the slow eastward evolution of the synoptic disturbance, may be conducive to high rainfall amounts.

At the beginning of October 2020, an intense extra-tropical cyclone (named Alex by MeteoFrance on behalf of EUMETNET, Brigitte in central Europe, and Aiden in the UK and Ireland) moved towards northern France, setting up the large-scale pattern typical of heavy rainfall over the western Alps, so that devastating floods occurred over the French Riviera, Liguria and Piedmont regions in Italy (C3S, https://climate.copernicus.eu/esotc/2020/storm-alex). As noted in a preliminary analysis of the event (Magnusson et al., 2021), the strong water vapour transport across the Mediterranean was organized in the form of an AR. The importance of mesoscale mechanisms of orographic interaction, associated with a moisture source from an AR, has been observed during intense orographic precipitation events over northern California (Smith et al., 2010) and the Pacific Northwest (Mueller et al., 2017).

Therefore, the aim of the present study is to analyse this torrential precipitation episode over north-western Italy building on the conceptual framework of heavy Alpine rainfall described above but evaluating also how the AR, which is a distinguishing aspect of this event, impacted on its severity and dynamics. For the first time, an identification algorithm is applied to objectively identify an AR coming from the North Atlantic, associated with heavy rainfall over the western Alps. The assessment of its role in triggering the severity of the event allows to add important additional details to the theoretical picture of heavy precipitation dynamical mechanisms in the area and to improve the understanding of the complex interaction between large scale flows and

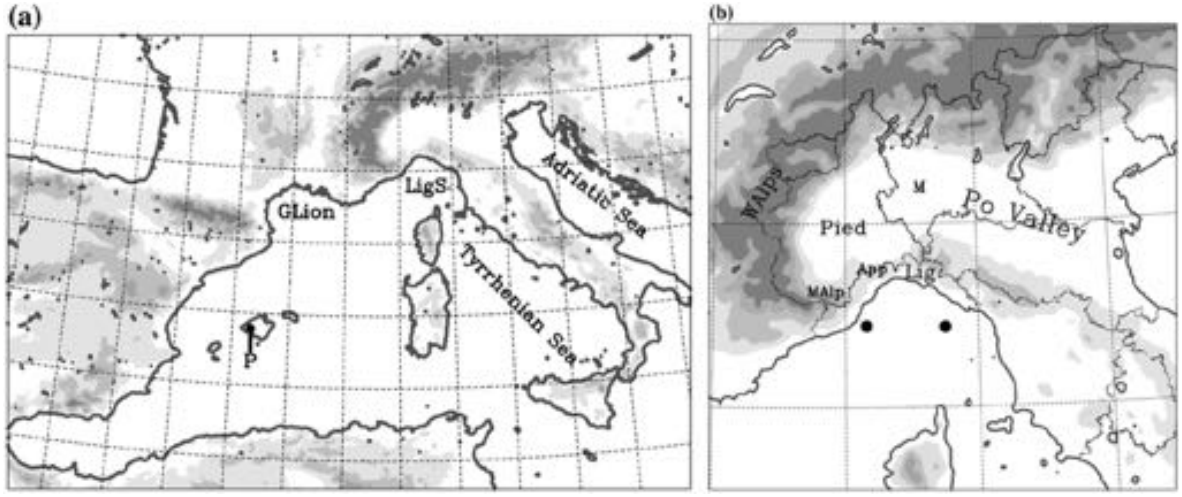

Fig. 1. Relevant geographical details of the area of interest and orography (grey shading corresponds to 500, 1000, 1500 and 2000 m). (a) MOLOCH integration domain; "GLion" and "LigS" indicate Gulf of Lion and Ligurian Sea, respectively; P indicates the location of the Palma sounding shown in Fig. 7. (b) Portion of the integration domain, "WAlps", MAlp" and "App" indicate the mountain areas of western Alps, Maritime Alps and Apennines; "Pied" and "Lig" indicate Piedmont and Liguria regions; M denote the location of Milan radiosounding shown in Fig. 8. The two black dots over the Ligurian Sea indicate the location where mixing ratio and moisture transport profiles are computed (see Section 4.2 and Fig. 13).

mesoscale dynamics during extreme precipitation events.

The paper is organized as follows. Section 2 provides an overview of the datasets and tools, including the numerical modelling chain. Section 3 describes the event, its ground effects and provides an evaluation of the AR intensity. Also, it analyses the moisture sources through backward trajectory computation. Section 4 presents the high-resolution simulation results devoted to investigate the mesoscale dynamical aspects and to evaluate the different contributions of water vapour transport to the severity of the event, their penetration towards the Alps and their interaction. Conclusions are drawn in Section 5.

2. Data, methods and tools

Different tools and methodologies are employed for a deep analysis of the multiscale features involved in the water vapour transport responsible for the severity of the case study. To investigate the large-scale transport, a Lagrangian perspective is adopted, computing 48-h backward trajectories through the Hybrid Single-Particle Lagrangian Integrated Trajectory (HYSPLIT) model (Stein et al., 2015; Rolph et al., 2017). HYSPLIT is applied to the Global Forecasting System (GFS) dataset, at 0.25-degree horizontal resolution and at 3-h intervals. The dataset is based on concatenated short-term forecast model output on native model (hybrid) levels from successive (6-hourly) GFS runs. Along the trajectories, ending at different elevations over the Alpine area affected by intense rainfall, moisture (relative humidity and mixing ratio) is considered.

The AR detection is based on the Guan and Waliser (2015) algorithm, which combines intensity and geometry thresholds. In fact, the AR is the object identified by contiguous areas that satisfy the following criteria: i) 85-percentile threshold for IVT, together with a minimum value (100 kg m^{-1} s^{-1}) that gets rid of weak-IVT areas; ii) length >2000 km and aspect ratio >2 (length/width). With respect to its original formulation, the algorithm required some adaptation because of the U-shape of the AR, originated over the Atlantic and entering the Mediterranean, and of the complex morphology of the basin. Thus, some modifications have been applied to the directional requirements of the algorithm. In more details, the threshold for coherence in IVT direction has been relaxed from 45° to 65° and the meridional component of IVT has not required to be strictly positive (northward). This allows for the identification of the AR as presented below in Section 3 and Fig. 3. For the AR detection, ERA5 reanalyses (Hersbach et al., 2020) provide IVT during the event and have been used for computing the monthly 85th percentiles of IVT over the last 15 years, as requested by the algorithm (Guan and Waliser, 2015). Moreover, ERA5 3-hourly IVT fields since 1959 to 2022 have been also used to compute percentiles, in order to provide a climatological context to this event (see Section 3) in the Mediterranean area.

Precipitation observations are provided by the ground-based rain gauges network managed by the regional offices and collected by the National Italian Civil Protection Department. This network is composed of about 4500 stations, and it is characterized by a mean density of 1/100 km^2, with higher resolution in the area of interest up to 1/50 km^2 (Bruno et al., 2021). Also, data provided within the event technical reports (ARPA Piemonte, 2020; ARPAL, 2020) available from the regional meteorological centres have been exploited especially for model validation (see Section 4).

This study exploits also high-resolution numerical simulations to better understand the interaction among the large-scale moisture transport by the AR, the mesoscale dynamics and the local complex orography. The BOLAM (BOlogna Limited Area Model)-MOLOCH (MOdello LOCale in Hybrid coordinates) modelling chain (Buzzi et al., 2014), developed at the Institute of Atmospheric Sciences and Climate of the Italian National Research Council (CNR-ISAC), is implemented using the European Centre for Medium-Range Weather Forecasts (ECMWF) analysis fields as initial and boundary conditions. Three different initialization times were adopted on the day before the event (0000, 0600 and 1200 UTC, 1 October 2020) to explore the variability of the predicted rainfall fields and identify a reference simulation for a detailed analysis. All the simulations lasted until 1200 UTC, 3 October 2020.

BOLAM is a hydrostatic limited-area model, which integrates the primitive equations on a latitude–longitude rotated grid (grid spacing about 10 km) and uses a terrain-following vertical coordinate system, in which the 50 sigma levels smoothly tend to a pressure coordinate far from the ground. Its domain covers the entire continental Europe up to 60°N and extends over tropical Africa till 20°N. To properly describe the evolution of the storm and of the vapour transport, the domain covers also a large part of the Atlantic Ocean. As in the current operational practice at CNR-ISAC, the convection permitting model MOLOCH (Malguzzi et al., 2006; Trini Castelli et al., 2020) is nested (one-way) in BOLAM. The latter provides the boundary conditions at a suitable temporal (hourly) resolution. The MOLOCH domain, consisting in 626 × 418 grid points with a horizontal grid spacing of about 3 km and 60 terrain-following vertical levels, covers the entire central-western Mediterranean basin (Fig. 1a). BOLAM and MOLOCH share the same three-dimensional advection scheme based on a second-order, weighted-average flux implementation with "superbee" limiter (Hubbard and Nikiforakis, 2003). Also, the physical parameterization schemes are similar, except for some adjustments due to the different nature and resolution of the models: boundary layer turbulence (E-l, 1.5 order closure; Zampieri et al., 2005; Trini Castelli et al., 2020), deep convection (Kain, 2004, not activated in the present application of MOLOCH), radiation (Ritter and Geleyn, 1992; Morcrette et al., 2008), and soil and microphysical processes (Buzzi et al., 2014). Orography, geographical distribution of soil types, soil physical parameters and vegetation coverage, as well as soil physical processes are described by means of a seven layers soil model. Sea surface temperature (SST) at the initial time is provided by the ECMWF analysis; then its evolution is based on a simple slab ocean model, where the deep ocean temperature is kept fixed, while SST evolves in the surface layer depending on radiative and latent/sensible heat fluxes. More details on the modelling chain can be found in Davolio et al. (2020b) and reference herein.

MOLOCH outputs are used to compute moisture fluxes along selected cross sections or vertical integrated values (from 1000 to 300 hPa) of water vapour (IWV) and IVT, defined as:

$$IWV = \frac{1}{g}\int_{sfc}^{300\ hPa} q\ dp = \int_{sfc}^{z_{300hPa}} \frac{q\ p}{R_d\ T_v}\ dz$$

$$\boldsymbol{IVT} = \frac{1}{g}\int_{sfc}^{300\ hPa} q\ \mathbf{V}\ dp = \left(\int_{sfc}^{z_{300\ hPa}} \frac{q\ u\ p}{R_d\ T_v}\ dz\ ;\ \int_{sfc}^{z_{300\ hPa}} \frac{q\ v\ p}{R_d\ T_v}\ dz \right)$$

where g is the gravitational acceleration, q the specific humidity, p the pressure, **V** (u,v) the horizontal wind (components), T_v the virtual temperature, and R_d the gas constant for dry air. Since the variables are defined on the model levels and not interpolated over isobaric surfaces, the integral is computed from the surface to the highest model level over which the pressure is lower than 300 hPa.

3. Synoptic evolution, precipitation and water vapour transport

The storm developed as a cut off low within an upper-level trough over the North Atlantic. An extra-tropical cyclone rapidly deepened west of Scotland on 1 October 2020 and the explosive cyclogenesis process (Sanders and Gyakum, 1980) was fostered by the dynamical interaction of the surface low with an intense jet stream characterized by a marked undulation over western Europe. The cyclone deepened to 970 hPa while moving south-eastward towards the Brittany coast where it first made landfall in the night between 1 and 2 October. During 2 and 3 October, the cyclone slowed its eastward progression across northern France, while the associated cold front swept over the Mediterranean basin, where heavy precipitation occurred. The storm Alex produced

hurricane force winds between southern UK and northern France, while heavy precipitation and thunderstorms severely affected south-eastern France and northern Italy (Mahovic and Nietosvaara, 2020; Magnusson et al., 2021), where numerous historical records of rainfall were broken and many floods occurred (ARPA Piemonte, 2020); outage of power, telecommunication, water supplies and rail services, infrastructure and environmental damages as well as at least 15 fatalities were the toll of this devastating weather event.

At 1200 UTC, 2 October (Fig. 2), a deep trough extended over the western Mediterranean and the intense pressure gradients along its southern border favoured strong water vapour transport in the form of an AR, located ahead of the cold front. The AR is clearly identified by the detection algorithm across the Atlantic Ocean, undulating north of the pressure ridge before descending southward, driven by the cyclonic circulation around the trough, and finally entering through the Gibraltar Strait into the Mediterranean basin (Fig. 3a). The AR pattern is also confirmed by the composite of Microwave satellite estimates of total precipitable water (Fig. 3b).

To contextualize the IVT of this event within the climatology of the western Mediterranean, all October IVT values since 1959 have been considered. The spatial variability of the 99.9th percentile for IVT is shown in Fig. 4a (note that the 85th percentile map is very similar to that shown by Lorente-Plazas et al., 2019 in their Fig. 2c). The 99.9th percentiles for IVT are larger over the sea, where values are generally lower than 800 kg m^{-1} s^{-1}, exceeding this threshold only over the Gulf of Lion and in the Ionian Sea. Therefore, since at its maximum intensity the AR analysed in the present study reached up to about 1120 kg m^{-1} s^{-1}, it ranks for sure in the top 0.1% in the western Mediterranean. In addition, Fig. 4b shows the maximum IVT values for each grid point of the domain in the same period, which range between 900 and 1200 kg m^{-1} s^{-1} over most of the western basin. The signature of the October 2020 AR can be clearly identified between Balearic Island and North Africa coast, indicating that IVT values in that area were the strongest ever recorded. Similarly, the AR associated with the October 2018 event analysed in Davolio et al. (2020a) left his footprint (IVT above 1200 kg m^{-1} s^{-1}) just over the central Italian coast (Fig. 4b). It is worth mentioning that these two ARs emerged in a preliminary climatological analysis, still ongoing, as among the five most intense events affecting northern Italy in the last 60 years, in terms of IVT values attained over the Mediterranean. Although IVT values were similar, the two ARs presented several differences. First a different remote origin, from North Atlantic in 2020 and from Tropical Africa regions in 2018. The persistence of the moisture supply and the extension of the area affected by moisture transport and by heavy precipitation were larger in 2018, while the AR analysed in this study was narrower and more focussed solely on western Italy. Finally, analysing the vertical distribution of moisture and moisture fluxes (see Fig. 6 in Davolio et al., 2020a), the AR analysed in this study was thicker, since the same high values of water vapour transport were confined below the lowest 4000 m in the 2018 storm, while reached higher elevation in October 2020.

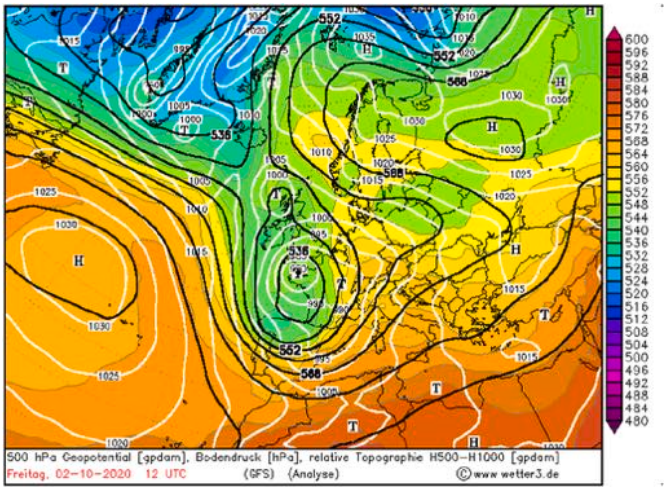

Fig. 2. GFS analysis of 500-hPa geopotential height (black contours), 500–1000-hPa thickness (colour shading), and mean sea level pressure (white contours) at 1200 UTC, 2 October 2020 (source www.wetter3.de). (For interpretation of the references to colour in this figure legend, the reader is referred to the Web version of this article.)

A further classification of the event is provided by the AR scale (Ralph et al., 2019; Eiras-Barca et al., 2021) that considers both the maximum instantaneous intensity at the landfall region and duration. Considering the Liguria coast as the landfall region in October 2020, since the maximum IVT in the area was about 950 kg m^{-1} s^{-1} and that the AR (as identified by the detection algorithm) remained over the region slightly longer than 24 h, the event falls in the AR3 (strong) category, very close to be AR4 (extreme). In 2018, considering the landfall over central Italy, the rank falls between AR4 and AR5.

At the mesoscale, the deepening trough activated a warm and moist low-level jet over the Tyrrhenian Sea impinging on the western Alps where it converged with an easterly current, entering from the northern Adriatic basin and flowing in the Po Valley along the Alpine foothills, as confirmed in the detailed description of the event by the Piedmont regional meteorological centre (ARPA Piemonte, 2020). Some rain gauge stations in the Piedmont region in Italy recorded their highest rainfall totals since records began in 1951. Precipitation amounts exceeding 600 mm, corresponding to an event with return time of more than 200 years, fell almost entirely during 2 October, although most of the rainfall occurred in the second half of the day, with maximum intensity in the late evening (Fig. 5c). Fig. 5a reveals two regions of heavy precipitation exceeding 200 mm in 24 h: over the Alps, where rainfall occurred over a wide area, and over the coastal orographic range (Apennines and Maritime Alps) of Liguria, close to the French border. Precipitation affected to a lesser extent, and especially in the morning of 2 October, also the eastern portion of Liguria. Finally, rainfall persisted in the same area in the very first hours of the day after, but quickly moved eastward with the cold front and weakened due to the arrival of cold and dry air over the area.

Compared to previous major floods, as those occurred in 2000 (Milelli et al., 2006), 2002 (Winschall et al., 2012) and 2016 (Cremonini and Tiranti, 2018), this event shares the same typical mesoscale pattern described above. On the other hand, the large-scale setting, although similar, presents some relevant differences. In fact, in previous episodes, the trough originated due to the intensification of a large amplitude baroclinic wave, producing a progressive increase of the pressure gradient between the western Mediterranean and eastern Europe, thus favouring meridional exchanges and a slow eastward progression of the weather systems. In October 2020, the trough was less pronounced over the western Mediterranean, and the cyclonic circulation was associated with an extremely intense storm over northern Europe, missing in the previous flood events. The baroclinic wave did not amplify markedly over the western Mediterranean and consequently resulted less stationary. Thus, the duration of the event was significantly shorter (but its severity was not lower), since the precipitation system swept over the area in about 24 h, while the previous floods were characterized by a greater stationarity of the phenomena. Thus, it seems important to investigate the role of the very intense AR, which appears as a peculiar feature of this event. Therefore, the first analysis aims at identifying the main sources of moisture feeding the extreme precipitation, through a Lagrangian backward trajectory computation as described in Section 2.

3.1. Trajectory analysis

To investigate the transport of moisture feeding the heavy precipitation system, backward trajectories are computed ending at different elevations in the Alpine portion of the Piedmont region, corresponding to the maximum rainfall area shown in Fig. 5a, and at different instants

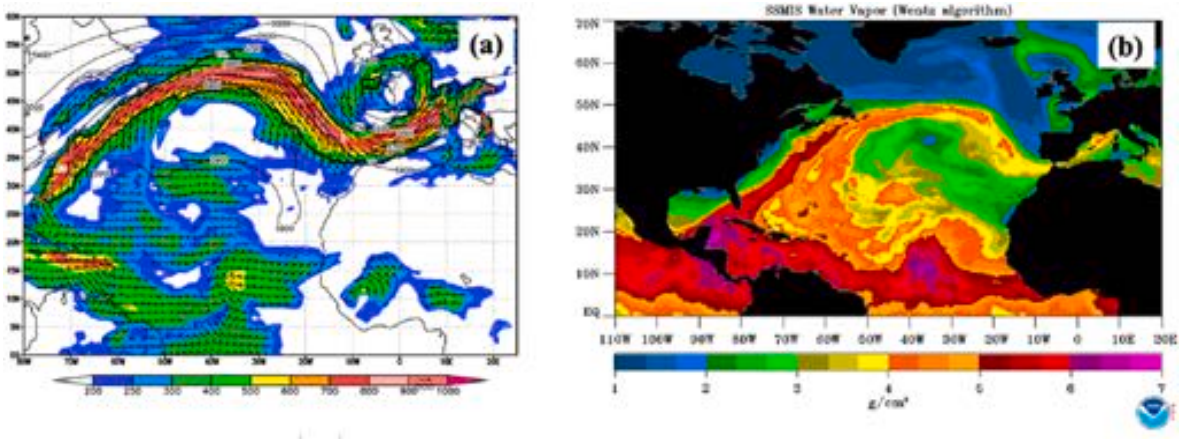

Fig. 3. (a) IVT (kg m^{-1} s^{-1}) and AR shape detection (thick black line), and 500 hPa geopotential height (gpm, thin black lines) at 1200 UTC, 2 October 2020. (b) Total Precipitable Water (g cm^{-2}) from SSM/I composite for 2 October 2020 (Image provided by the NOAA/OAR/ESRL PSL, Boulder, Colorado, USA, from their website at http://psl.noaa.gov/).

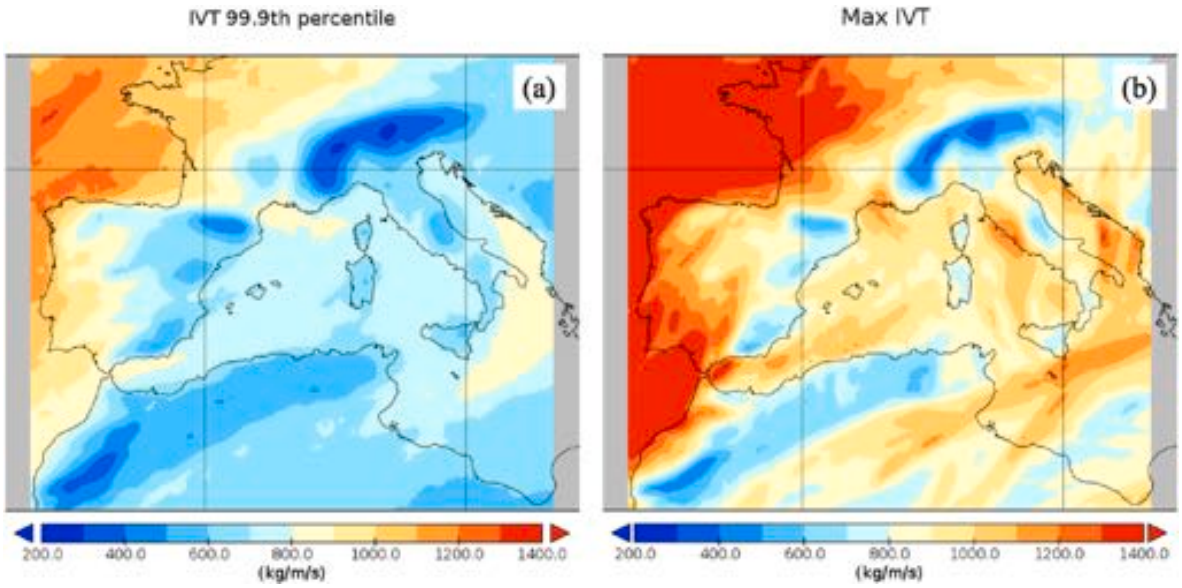

Fig. 4. (a) 99.9th percentile and (b) max values of IVT (kg m^{-1} s^{-1}) for October in the period 1959–2022.

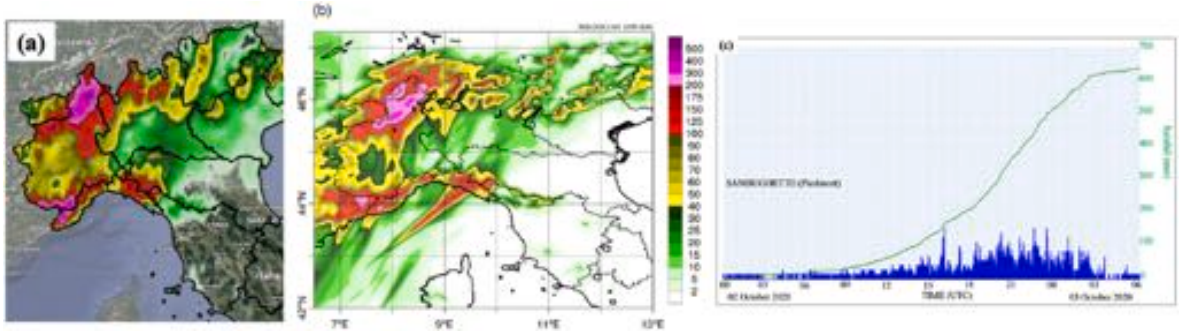

Fig. 5. The 24-accumulated precipitation (mm) during 2 October 2020. (a) Interpolation of the Italian rain gauge network; the rainfall map is provided by the National Civil Protection Department through the Dewetra platform (Italian Civil Protection and CIMA Research Foundation, 2014). (b) As simulated by MOLOCH; the displayed area is a small portion of the entire integration domain. Administrative borders among the Italian regions are also shown. (c) Rainfall time series at the station where the highest precipitation amount was recorded (Sambughetto in the Piedmont region over NW Alps, provided by the Dewetra platform).

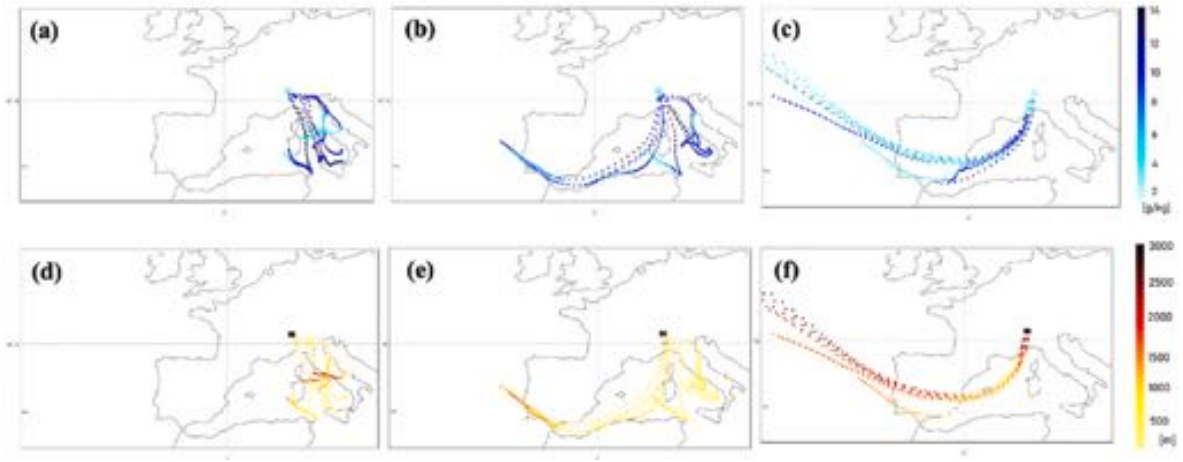

Fig. 6. Set of nine 48-h backward air parcel trajectories, computed using the HYSPLIT model, ending at 0000 UTC, 3 October 2020 over the western Alps in the area of maximum precipitation at different elevation a.s.l.: (a, d) 2500 m, (b, e) 3000 m and (c, f) 4000 m. (a, b, c) show air parcel mixing ratio (g kg^{-1}); (d, e, f) show the air parcel elevation (m a.s.l.).

in the afternoon of 2 October. Fig. 6 shows the results of three groups of nine 48-h backward air parcel trajectories that end at 2500, 3000 and 4000 m a.s.l. (above sea level), respectively, at 0000 UTC, 3 October. It is worth mentioning that the GFS orography elevation in correspondence to the nine ending points does not exceed 2500 m and that, changing the ending time to other instants within the most intense phase of the event, that is in the afternoon of 2 October, leads to almost the same results.

Air parcels reaching the Alps at 2500 m a.s.l. originate entirely over the central Mediterranean (Fig. 6a,d). Some of them move northward over the Tyrrhenian Sea at low elevation (less than 500 m a.s.l.) while moistening (mixing ratio between 10 and 12 g kg^{-1}) possibly due to turbulent mixing in the moist marine boundary layer, until they are forced to rise suddenly over the Apennines and the Alps. The passage over the orography produces an increase of the relative humidity up to saturation, and a progressive drop of water vapour content, indicating condensation and precipitation along the final part of the trajectories. The same effect of condensation is evident for those particles that overcome the central Apennine, move northward over the Adriatic Sea, where they gain moisture, and finally enter the Po Valley (barrier wind described in Section 1).

The analysis of trajectories ending at a higher elevation over the Alps (3000 m, Fig. 6b,e) identifies two different regions of origin of the parcels. Half of the trajectories display the same characteristics described above as they travel over the Tyrrhenian or the Adriatic Seas, reaching the easternmost portion of the precipitation area. The others originate far away over the Atlantic Ocean, where they travel at a relatively high elevation, above 1500 m a.s.l. These parcels descend as they enter the Mediterranean basin (even below 500 m a.s.l.) and experience a marked increase of mixing ratio from 5 to 8 to more than 10 g kg^{-1}, before being lifted over the Italian orography where precipitation occurs.

Air parcels ending at higher elevation (4000 m a.s.l., Fig. 6c,f) originate exclusively from the Atlantic Ocean (note that the same behaviour is observed already at 3500 m a.s.l.) where they travel above 2000 m a.s.l. and are characterized by mixing ratios often below 5 g kg^{-1} (the higher the elevation, the lower the moisture). Again, when this flow enters the Mediterranean basin in correspondence of the southern tip of the Iberian Peninsula, the parcels get closer to the sea surface and experience an increase of moisture content.

The present analysis, besides providing an insight on the sources of moisture feeding the heavy rainfall, reveals that there are three main paths towards the precipitation area, and that these three feeding flows superimpose each other before reaching the Alps: the easterly flow from the Adriatic moves at the lowest elevation, while, at higher altitudes, the southerly flow from the Tyrrhenian Sea progressively leaves room to the southwesterlies from the Atlantic and the western Mediterranean. The latter dominates above 3500 m a.s.l.

For clarity's sake, the results shown so far refer to a very limited number of trajectories, but they have been checked using a much denser matrix of grid points corresponding to the end of the trajectories. For each level, more than one hundred parcels have been computed to identify the three clusters of trajectories, with only some "outliers" (trajectories that do not pertain clearly to any of the three clusters). Although the water vapour amount of the parcels that reach the coastline is quite similar and in the range 10–12 g kg^{-1}, with slightly lower values for the trajectories coming from the Adriatic, the parcels coming from the Atlantic area display the largest variation in mixing ratio, since their descent over the Mediterranean basin allows to increase the moisture, due to exchange with the moist boundary layer, but also probably to convergence. In fact, not only the trajectories closer to the sea surface experience an increase in humidity, but also those that remain at higher level. In any case, the lower the trajectory altitude over the Mediterranean, the larger the mixing ratio increase, suggesting a role of the sea surface.

4. High resolution numerical simulations

Despite the relatively coarse resolution, GFS and ERA5 data, and consequently HYSPLIT trajectory analysis, have allowed to confirm the transport of humidity in the form of an AR and to describe the general dynamical picture of the moist flows feeding the precipitation, in good agreement with the preliminary study of Magnusson et al. (2021). In order to gain a more detailed view of the mechanisms responsible for extreme rainfall, high resolution is required; therefore, numerical simulations with the convection permitting model MOLOCH (see Section 2) have been performed. Since our aim is to exploit these high-resolution numerical experiments to closely examine the mechanisms of water vapour penetration across the orography and the mesoscale dynamics, it is first necessary to verify that the model output is in general agreement with the observations, especially as far as rainfall and moisture fields are concerned. A detailed quantitative validation of the model is out of the scope of the present paper; however, as discussed hereafter, the simulations turn out to correctly reproduce the distribution of the precipitation and the main dynamical patterns of the event.

The three MOLOCH simulations, initialized 6 h apart since 0000 UTC on 1 October, reproduce quite accurately the 24-h accumulated rainfall on 2 October and differ only slightly from each other. However, the

simulation starting at 1200 UTC produces the most intense rainfall peaks (Fig. 5b) and looks much closer to the observations. For example, it is the only numerical experiment that correctly reproduces the rainfall band over the sea on the eastern portion of the Genoa Gulf in the early morning of 2 October (caught by radar, not shown), due to convective activity organized along a low-level convergence line and triggered by moderately unstable moist prefrontal flows. Therefore, only this simulation, taken as the reference, is discussed and used to investigate the physical mechanisms.

Compared with the observed daily rainfall (Fig. 5a), the two areas of intense precipitation are well defined. Over the Apennines and Maritime Alps, the maximum intensity is attained close to the French border and in correspondence with the mountain crests, confirming the mainly orographic nature of the precipitation (even though some convective activity was present, as demonstrated by lightning detection). Moreover, the area of low precipitation almost in the middle of the Liguria region is correctly placed. Rainfall markedly decreases moving southward towards the coast as well as northward over the Po Valley and affects only the western portion of the plain. Finally, the most intense precipitation is correctly localized over the western Alps, although the model underestimates the peaks, which reach almost 400 mm in 24 h in some limited regions. In any case, the wide area most severely affected by torrential rainfall, with amount exceeding 200 mm, is correctly outlined. It is worth noting that also the rainfall field simulated by BOLAM correctly captures the main patterns, although the field appears much smoother, and the peaks largely underestimated especially over the Apennines where the value of 200 mm is hardly reached.

The water vapour transport over the Mediterranean is among the important characteristics of the event that the model should be able to reproduce realistically for a correct simulation of the rainfall field. To this aim, the vertical thermodynamic profiles of the atmosphere at the Palma station on the Balearic Islands are analysed to verify that the model simulates the correct timing of the arrival of the AR from the Atlantic into the Mediterranean basin. Observations at 0000 UTC, 2 October (Fig. 7a), reveal a quite dry and moderately unstable atmosphere, on top of an almost saturated and calm boundary layer, capped by an inversion at 900 hPa that strongly inhibits convective triggering. However, just 12 h later (Fig. 7b), the approach of the AR is revealed by a pronounced increase of humidity especially in the lower and middle troposphere between 850 and 500 hPa, pushed by south-westerly winds. Finally, at 0000 UTC on the following day (not shown), behind the cold front, the dry air trapped within the cyclonic circulation of the storm

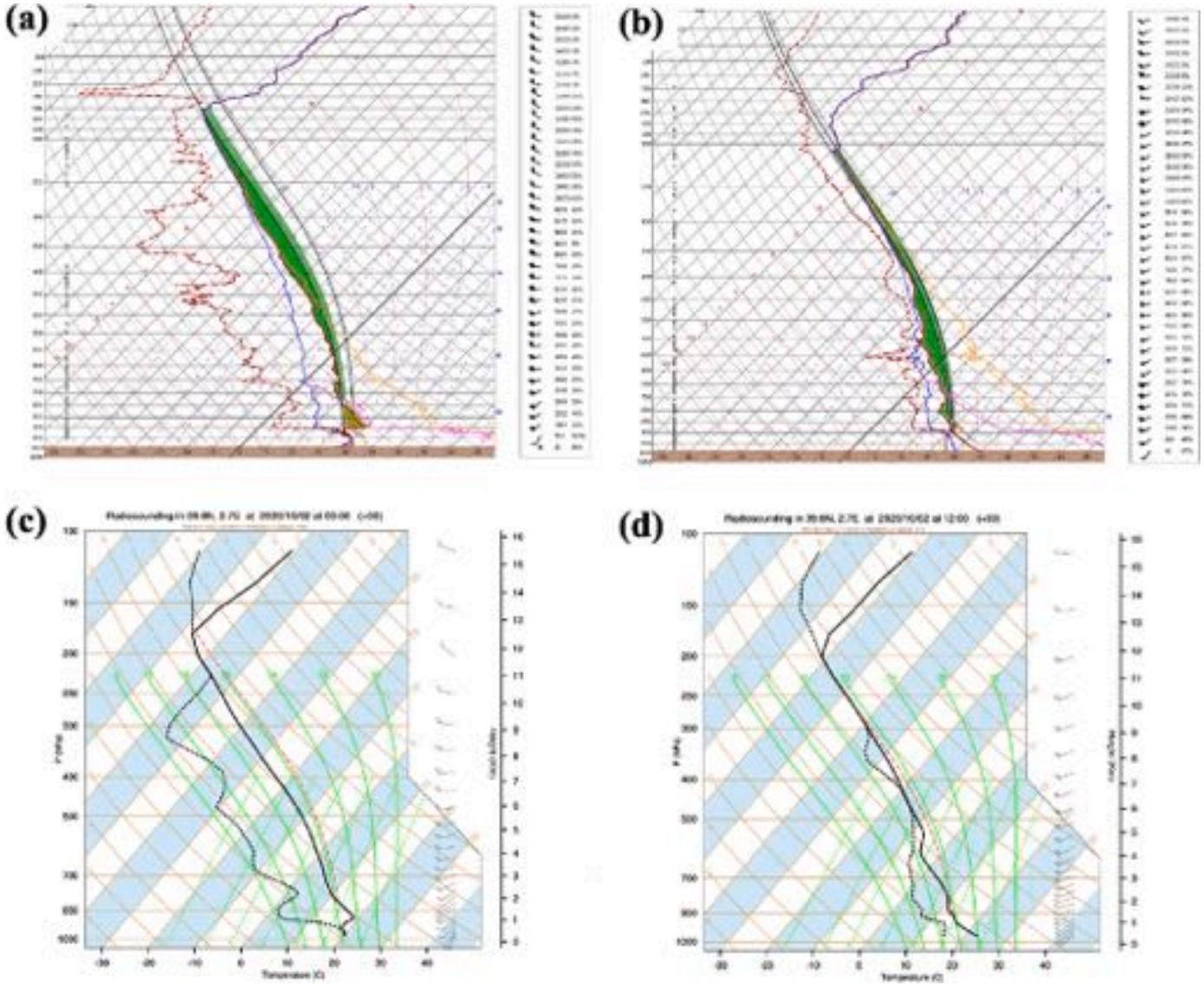

Fig. 7. Skew T/log P thermodynamic diagrams at 0000 UTC (a, c) and 1200 UTC (b, d) 2 October 2020, as measured (a, b, *source AEMET*) and computed from the MOLOCH simulation (c, d) at Palma de Mallorca (code 08 302 – location shown in Fig. 1a).

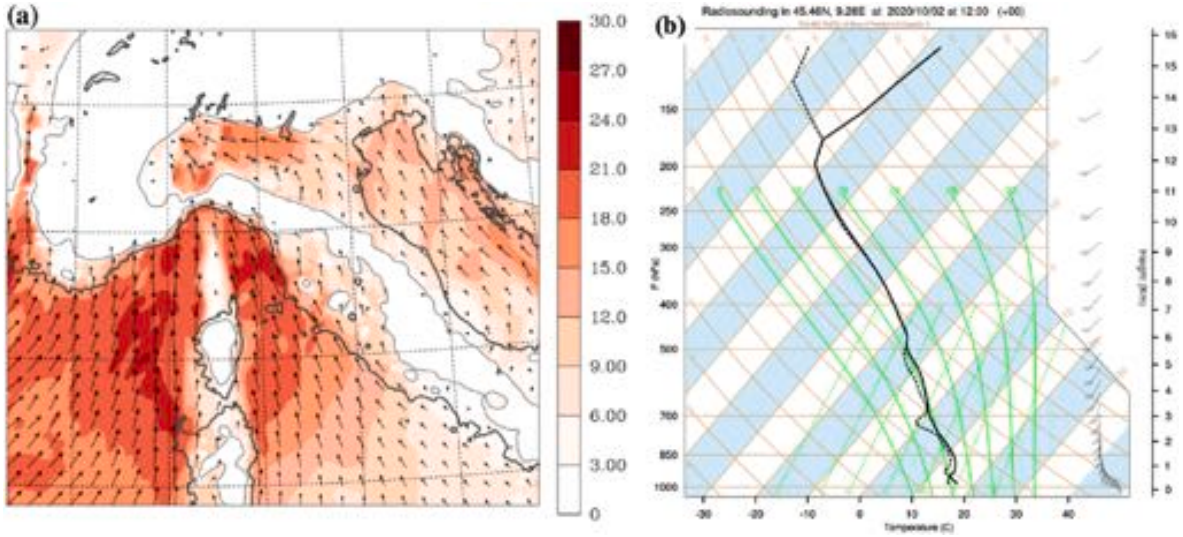

Fig. 8. (a) 950-hPa wind as simulated by MOLOCH at 1200 UTC, 2 October 2020; grey contour shows the 500 m orography elevations. (b) Skew T/log P thermodynamic diagrams at Milan, computed from MOLOCH simulation at 1200 UTC, 2 October 2020 (code 16 080 – location shown in Fig. 1b).

Alex enters the western Mediterranean and produces a clear moisture drop in the middle troposphere. Also, an evident lowering of the tropopause is revealed in the skew-T diagram. All these characteristics of the atmospheric profiles are well reproduced in the MOLOCH simulation (Fig. 7c and d) indicating that the AR entrance in the basin is correctly captured by the model.

Data from GPS ground sensors along the western Mediterranean coast from Spain to Italy, including islands, have been also used to compare the total column water vapour content (not shown), confirming a good timing of the simulated moisture field evolution over the whole Mediterranean area.

4.1. Dynamical mechanisms and moisture transport

Focusing on north-western Italy, the high-resolution simulation (Fig. 8a) clearly shows the convergence over the Alpine foothills of the easterly (barrier) flow over the Po Valley with the southerly moist currents from the sea (as revealed by the analysis of the backward trajectories in Section 3.1), favoured by the orographic configuration. A similar low-level convergence was observed during the 1994 Piedmont flood and was considered as a key ingredient of the heavy rainfall episode (Rotunno and Ferretti, 2001). This pattern remains almost unchanged since the early morning of 2 October to the end of the event, although the intensity of the southerly currents progressively increases, attaining its maximum in the late evening. The southerly flow appears as composed by two different branches: one from south/southwest, flowing to the west of Corsica and associated with the AR, the other one from south/southeast, over the Tyrrhenian Sea. The weak wind area at 950 hPa in the lee side of the Apennines, over the western corner of the Po Valley, indicates that the southerly currents, especially the westernmost ones, rise above this level and over the low-level easterly flow as soon as it overtakes the Apennine crest. On the other hand, the easterly current, which can be clearly identified in the middle of the Po valley (Fig. 8a), seems very intense at this level and possibly undercuts the southerly flow. In fact, the simulated radiosounding in Milan at 1200 UTC, 2 October (Fig. 8b), which is in close agreement with the observations (not shown), describes a nearly saturated, moist neutral atmosphere characterized by intense south-westerly winds above 850 hPa, but in the lowest 1500 m the wind abruptly rotates becoming easterly and colder air is trapped in the boundary layer.

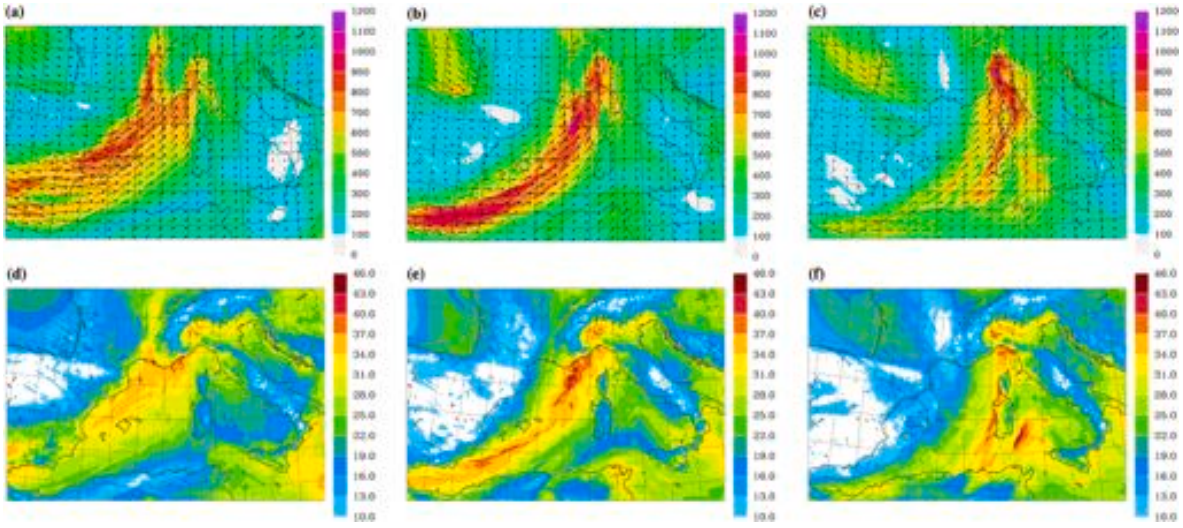

Fig. 9. IVT (a, b, c) in kg m^{-1} s^{-1} and IWV (d, e, f) in kg m^{-2} or mm simulated by MOLOCH at (a, d) 1200 and (b, e) 1800 UTC on 2 October, and (c, f) at 0000 UTC on 3 October 2020.

The investigation of the moisture transport is necessary to quantify the role of each impinging flow in the heavy precipitation. At 1200 UTC, 2 October, the IVT simulated by MOLOCH (Fig. 9a) shows that the AR passes over the Iberian Peninsula, and it is already affecting the western Alps with its eastern branch, although its core (about 800 kg m^{-1} s^{-1}) over the Mediterranean is directed towards southern France, where floods actually occurred. A wide area of high values (up to 40 mm) of IWV (Fig. 9d) extends from the Balearic Islands to the Gulf of Lion and the French Riviera. At 1800 UTC (Fig. 9b,e), the structure of the AR progresses eastward and becomes more definite over the Mediterranean, and a narrow band of high (40–45 mm) IWV lies from the Gibraltar Strait to northern Italy. The moisture transport attains its maximum, with simulated values slightly above 1300 kg m^{-1} s^{-1} upstream of the Ligurian coast, a value comparable with that of the AR during the extreme event of October 2018 (Davolio et al., 2020a). A rather intense moisture transport activates also north-east of Corsica, over the Tyrrhenian Sea, due to the high atmospheric moisture content (IWV of 30–35 mm) and intense low-level wind. At this time, the band of high IVT clearly penetrates over north-western Italy and a marked decrease appears as it crosses the Alps. The northward elongation is confirmed also by the high values of IWV over the western Po Valley (up to 40 mm), between the Apennines and the Alps. Finally, as the cold front sweeps the western Mediterranean, pushed by cold and dry Mistral on its back, the AR axis rotates becoming more meridionally aligned (Fig. 9c,f), and the moisture transport focuses on the eastern Liguria coast, while still affecting the same area over the western Alps, where in fact major floods occurred. At this time, although the corridor characterized by high moisture content over the Mediterranean does not seem to be still connected with the reservoir over the Atlantic, high IVT values persist, mainly due to the intensification of the low-level jet ahead of the cold front. As the front moves eastward, the severe weather quickly comes to an end.

The time integrated IVT over the 24 h of 2 October, almost corresponding to the entire life cycle of the AR in the Mediterranean, clearly reveals (Fig. 10) the main corridor of water vapour from the Atlantic area, through the Mediterranean basin, directed towards the Alps. Interestingly, the region of intense precipitation over northern Italy (indicated by the 200 mm black contour line in Fig. 10) is located right to the north of the core of the time integrated IVT.

4.2. Penetration of the water vapour

The strong advection of water vapour from the south offshore the western Italian coast is described in Fig. 11, which shows the evolution of the water vapour flux across five longitudinal cross sections, located (Fig. 11b) between the northern tip of Corsica (43°N) and the northern side of the Alps (about 47°N), upstream and downstream of the area affected by the heaviest rainfall. The moisture flux constantly increases with time since the evening of 1 October, peaking in the afternoon of 2 October, around 1800 UTC, when the AR reaches its maximum intensity. The flux does not change between the two southernmost sections A and B, since precipitation is not relevant over the sea. In contrast, the water vapour flux through section C shows the effects of the first forced ascent of the moisture-laden flow, and especially of the AR, over the Apennine orography. The peak value through C is much less than across the upstream sections as water vapour condenses and precipitates in the form of rain. Also, a slight decrease is observed travelling over the Po Valley from section C to D. This is probably due not only to the relatively weak precipitation over the plain, but also to rainfall over the Alpine area next to the western Italian border. However, the strongest depletion of water vapour occurs crossing the Alps. It is there that a relevant amount of moisture is converted into precipitation and the flux peak in section E is almost halved with respect to the sections offshore. The amount of vapour removed from the impinging cross-barrier air-mass can be estimated integrating in time the vapour flux across the sections during the event. The moisture depletion due to crossing both Apennines and Alps is around 40%, while moving from section C to E across the Alpine chain produces a drying ratio between 25 and 30%. These values are to be considered indicative, since the sections are not perfectly suitable for calculating the drying ratio: in fact, they do not intercept strictly the same water vapour flux (recall that the flow in the upper troposphere is southwesterly), and they are not always parallel to the Alpine chain which has a complex shape in western Italy. However, the values obtained are well within the expected range computed for different mountain ranges (Smith et al., 2010) and for the Alps in particular (Smith et al., 2003).

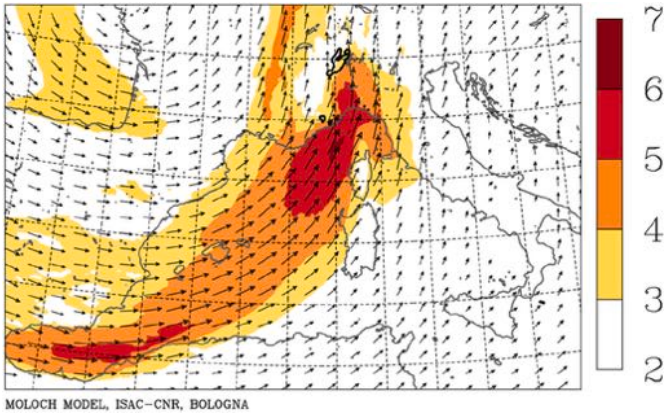

Fig. 10. IVT (shaded in 10^7 kg m^{-1}) integrated in time during 24 h on 2 October 2020. The 200 mm rainfall contour over north-western Italy is shown in bold black line.

Therefore, as the AR progressively intensifies and becomes narrow, it reaches the Italian coast, and the moisture is transported towards the Alps where orographically forced uplift triggers condensation and heavy precipitation. As seen above, a relevant amount of moisture impinges the Alpine divide also coming from the Tyrrhenian Sea. The latter transport is due to the low-level jet, that is typically associated to heavy precipitation events over western Alps (Buzzi and Foschini, 2000; Davolio et al., 2020b). The penetration of the moisture towards the Alps along these two corridors can be further analysed exploiting the high-resolution numerical simulations and analysing the moisture transport along the vertical sections (Fig. 12), respectively from SW to NE along the main axis of the AR, from SE to NW along the moisture contribution from the Tyrrhenian Sea. Moreover, a section is also drawn along the Po Valley to describe the contribution coming from the Adriatic (sections placement is shown in Fig. 11b). This allows also to further investigate the dynamical interaction among the three different contributing flows.

In the morning of 2 October, at 0900 UTC (Fig. 12a) the first offshore water vapour tongue from the southwest reaches the Liguria coast and is lifted over the Apennines. The intense vertical velocity indicates possible development of convection over the crest, consistent with a more potentially unstable atmosphere at the beginning of the event. At the same time, some moisture is coming also from the Tyrrhenian Sea and from the Adriatic (Fig. 12 d, g), but fluxes are considerably lower especially due to weaker low-level winds. By 1800 UTC (Fig. 12b), the AR has already crossed the Apennines and is lifted over the Alps where intense precipitation occurs. The intense vertical velocity suggests the possible presence of convective activity embedded within the orographic stratiform precipitation. Using the 150 kg m^{-2} s^{-1} isoline as reference (switching from yellow to blue in the figures), the thickness of the moist flow over the sea reaches 2 km. The moist flow that crosses the Apennines appears as an elevated region of water vapour travelling towards the Alps over the Po Valley, that does not descend close to the surface. However, only a small portion of this vapour can cross the Alps. The southerly flow from the Ligurian Sea (Fig. 12e) displays a similar behaviour while crossing the Po Valley, although its core is located

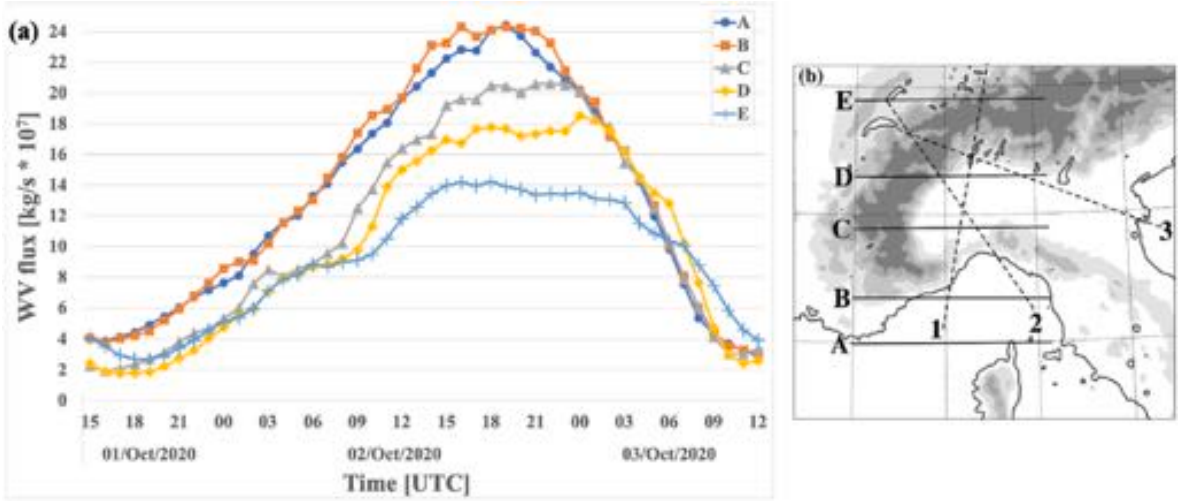

Fig. 11. (a) Time series of WV fluxes (kg s^{-1}) across the sections A-to-E displayed in (b). In (b) are also drawn the vertical sections (1, 2 and 3) displayed in Fig. 12.

slightly below, around 1 km from the ground. Over the sea the moisture flux is confined in a much thinner layer (almost halved) with respect to the AR, whose depth is slightly above 1 km (same reference of the 150 kg m^{-2} s^{-1} isoline). However, due to the intense low-level jet, the peak intensity of the flux along this section is comparable to that attained along section 1. On the other hand, the easterly moist air, that flows parallel to the Alps from the Adriatic basin (Fig. 12h), wedges underneath the southerly flows in the lowest layers over the Po Valley, being also characterized by a much lower equivalent potential temperature (not shown). Fig. 12c shows the arrival of dry air, at the end of the day, over the western portion of the Genoa Gulf in the lower troposphere, in the rear of the cold front. The AR moves eastward (see also Fig. 9c) and merges with the flow from the Tyrrhenian Sea (Fig. 12f), which in this phase becomes the main contribution of moisture to the precipitation. Also, the easterly flow in the low level over the plain maintains its magnitude and possibly contributes to retard the eastward movement of the precipitation system, which persists on the Alps (as suggested also in previous studies as Rotunno and Ferretti, 2001).

The analysis of the water vapour flux along the three different directions has allowed to identify the different characteristics of the moist flow associated with the AR with respect to the low-level jet east of Corsica. Moreover, it has clearly confirmed the convergence of the three contributions, as in the general picture presented by Rotunno and Ferretti (2003), that possibly enhances the orographic uplift over the Alps.

To better quantify the differences between the two southerly currents directed towards the Alps, their characteristics in terms of mixing ratio and moisture transport profiles are sampled upstream, over the Genoa Gulf, before being disturbed by the presence of the orography. Two points (their position is shown in Fig. 1b) are selected at the same latitude 43.88°N, at 8.35°E and 9.50°E respectively, where vertical profiles are computed, using the meteorological variables averaged over an area of about 15 km × 15 km around each point. Time-averaged 6-hourly mixing ratio profiles (Fig. 13 a,b) show the evolution of the moisture content over the western and eastern Ligurian Sea, characterizing the two branches of the impinging flow. The atmospheric column shows high humidity content already in the early morning since the prefrontal moist flow has already started and feeds the convective activity over the sea. However, as the AR approaches, the depth of the moist layer increases: while the maximum value close to the surface does not change, the mixing ratio becomes larger in the layers above, up to about 2000 m, and in the middle troposphere. The same values are kept until the end of the event, marked by the abrupt drop of moisture in the morning of 3 October.

Comparable values of water vapour mixing ratio at the surface are shown in the eastern side of the Ligurian Sea, although a steeper decrease occurs especially in the first 1000 m. This is consistent with the different thickness of the moist layer impinging the Apennines, as shown in Fig. 12. The highest moisture content here is reached in the evening of 2 October, after 1800 UTC, and the decrease in the morning of 3 October is weaker due to the progressive shift of the AR over this area, as shown in Fig. 9e and f, which is also responsible for the increase of moisture in the middle troposphere in this phase.

The 6-hourly averaged water vapour flux profiles (Fig. 13 c,d) notably differ from those of mixing ratio due to the influence of the wind. On the west side, water vapour transport values are largest just below 1000 m, and the elevation of the peak slightly lowers during the day. The most intense transport over the deepest layer is attained in the early afternoon, between 1200 and 1800 UTC. Later in the evening, the increased transport in the middle troposphere, between 2000 and 5000 m, is due to the intensification of south-westerly winds just ahead of the approaching cold front. On the eastern side a different behaviour is depicted: the moisture transport peak elevation is initially lower, around 500 m, and increases during the day, with the maximum intensity reached in the evening. This reflects the presence of a low-level jet over the Tyrrhenian Sea which becomes "contaminated" by the AR during the last hours of 2 October and the next morning. As seen on the western side, the depth of the moist layer increases due to water vapour transport in the middle troposphere, but with some hours of delay. Therefore, a fair comparison between the characteristics of the two southerly branches, the AR and the low-level jet, can be performed between 0600 and 1800 UTC, before they superimpose. Within this time frame, the vertical profiles confirm a much thicker column of moist air and moisture transport associated with the AR, although the maximum intensity of the transport is comparable. This reveals strongest winds associated with the low-level jet on the eastern side.

4.3. Sensitivity experiments

An additional numerical experiment is devised to evaluate, at least qualitatively, the contribution of the AR to the precipitation. The idea is to exploit the numerical model as a virtual laboratory used to analyse what happens if we get rid of the moisture transported into the Mediterranean by the AR. Since the boundary of the MOLOCH domain is placed in correspondence of the Gibraltar Strait, it intercepts the AR entering the Mediterranean. Therefore, a drastic reduction (75% of its original value) of the moisture entering the western border of the integration domain allows to significantly weaken the AR and its moisture transport. It is worth specifying that this percentage was subjectively chosen to markedly weaken the AR transport and that the modification is applied only to the southern portion of the western boundary, in order

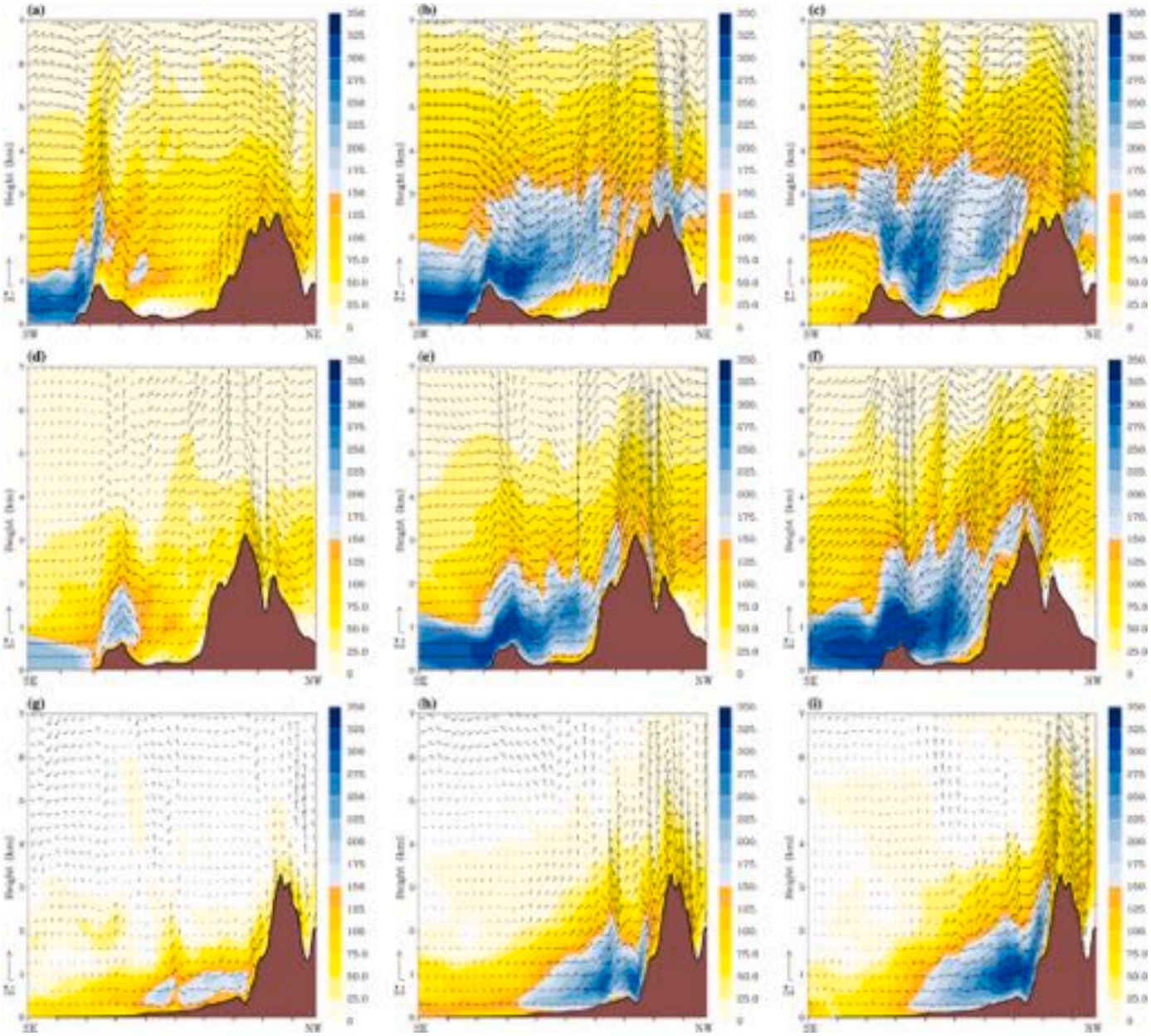

Fig. 12. WV fluxes (kg m^{-2} s^{-1}) along the vertical sections shown in Fig. 11b, valid on 02 October at 09 UTC (a, d, g), 18 UTC (b, e, h), and 03 October at 00 UTC (c, f, i). Section 1 (a, b and c) along the AR, section 2 (d, e and f) over the Tyrrhenian Sea and section 3 (g, h and i) across the Po Valley. Note that the scale of horizontal and vertical wind components is different, as shown by the vectors drawn on the bottom-left side of each panel.

to modify the AR intensity but limiting the perturbation to the rest of the simulation. The nesting procedure imposes the BOLAM model fields on the external frames of the MOLOCH domain every hour. All the boundary conditions are thus modified accordingly (reducing moisture) only in correspondence of the selected part of the boundary.

As expected, since the modification is applied only to a limited portion of the boundary, the evolution of the pressure fields over Europe in the sensitivity simulations is almost unchanged and the synoptic patterns do not differ from those of the control run. This favours a fair comparison between the two experiments. Of course, over the Mediterranean the moisture field is profoundly altered as shown in Fig. 14 in correspondence with the timing of maximum intensity of the AR (compare with Fig. 9b,e). Although the winds are still strong in the sensitivity simulation, the low amount of water vapour, except for the area closer to the Italian coast, critically reduces the IVT and the AR is not detectable anymore over the Mediterranean.

Fig. 15 reveals the impact on the precipitation and provides a clue on the role of the AR. The rainfall is almost unchanged between 0000 and 1200 UTC of 2 October, when the AR has not started yet to contribute to the pre-frontal south-westerly flow reaching the Italian coast. Differences between the precipitation fields (Fig. 15e) can be ascribed mainly to shift in the pattern and are limited to a few tens of mm. On the other hand, in the afternoon, the difference between the two experiments is significantly larger. A slight increase of the rainfall over the Po Valley and the central-eastern portion of the Apennines (no more than 50 mm/12h) in the sensitivity simulation is possibly due to the different interaction between the southerly flows. However, the relevant result is that the sensitivity simulation produces a much weaker precipitation all over the western Italy, up to almost 250 mm/12h less than the CNTR run. The same dynamical mechanisms described in previous sections are in place, but the lack of the moisture contribution by the AR almost halves the amount of rainfall over both the Apennines and the Alps. Therefore, it

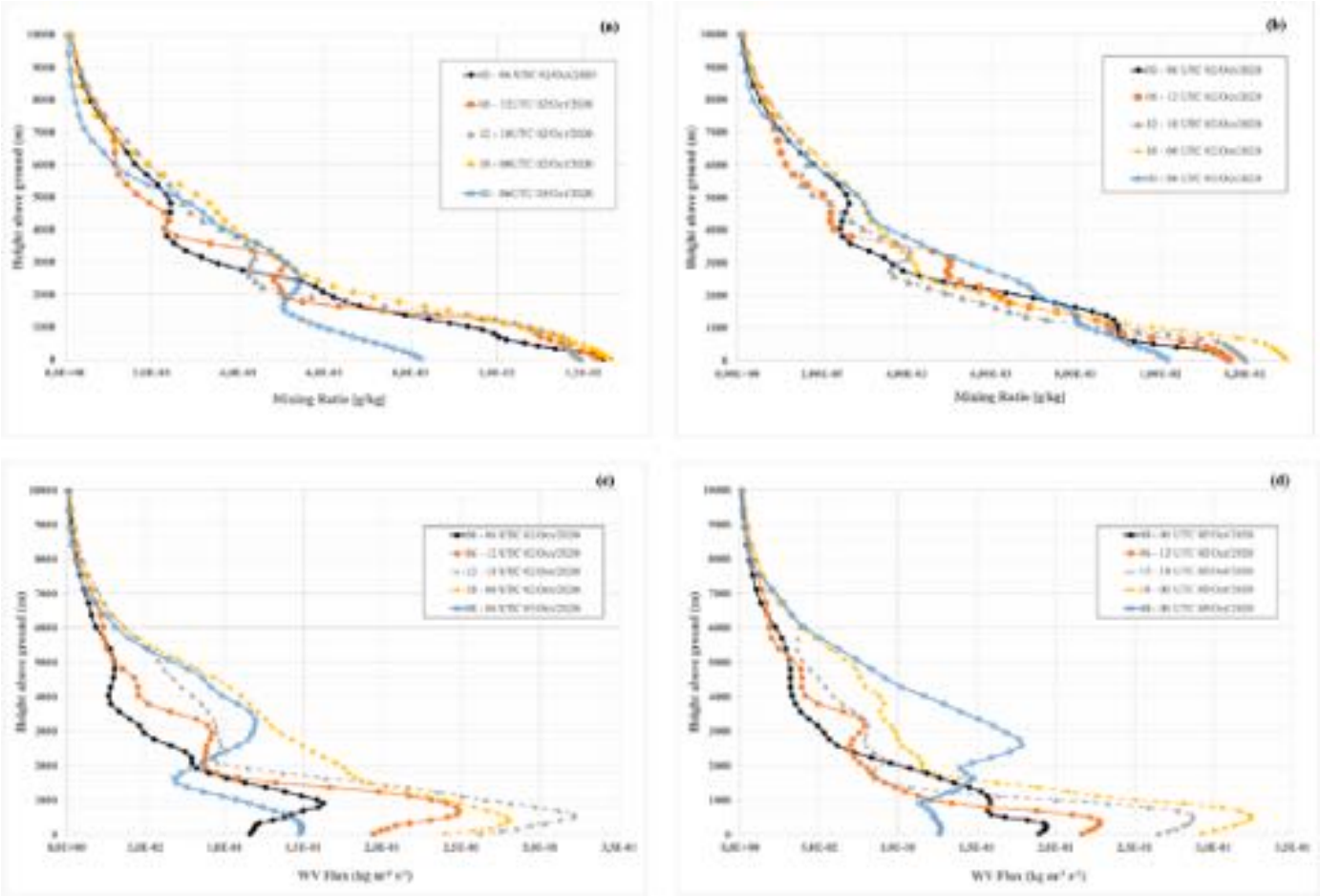

Fig. 13. vertical profiles of (a, b) mixing ratio (g/kg) and (c, d) WV flux (kg m^{-2} s^{-1}) computed from the MOLOCH simulations in two points over the Gulf of Genoa (Ligurian Sea – location shown in Fig. 1b) at 43.88°N, and 8.35°E (a, c) and 9.50°E (b, d), respectively. Profiles are averaged over 6 h.

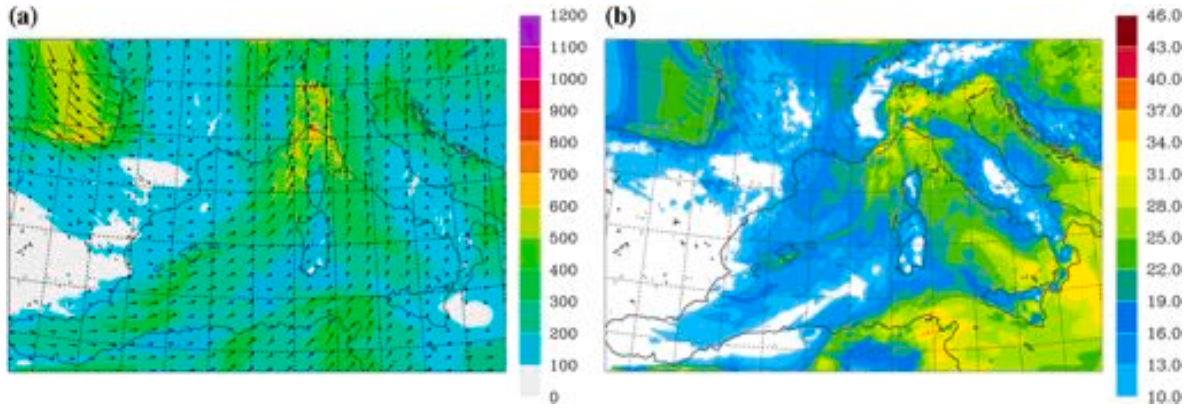

Fig. 14. IVT (a) in kg m^{-1} s^{-1} and IWV (b) in kg m^{-2} or mm simulated by MOLOCH at 1800 UTC, 2 October 2020 in the sensitivity numerical experiments.

turns out that the AR is critically important: the extreme event, without the AR, would have become an "ordinary" intense precipitation event, also because, unlike previous historical flood events in this region, the synoptic evolution is less stationary and thus the precipitation system rests over the area only for 24 h.

5. Conclusions

The present study has analysed in detail a recent heavy precipitation episode occurred over the southern side of the Alps. At the beginning of October 2020, an early-season explosive extratropical cyclone, named Alex, was responsible for windstorms over UK and France, and the associated trough extending over the Mediterranean produced favourable conditions for torrential rainfall over southern France and western Italy. Over the Alpine area, orographic precipitation lasted a little more than 24 h, during 2 and 3 October, mostly concentrated in about 12 h in the evening of the first day. In several rain gauge stations of Piedmont region, this resulted in record-breaking rainfall totals in the last 70 years. This particular case was chosen not only for its extreme severity, but especially for its similarity, in both the synoptic conditions and

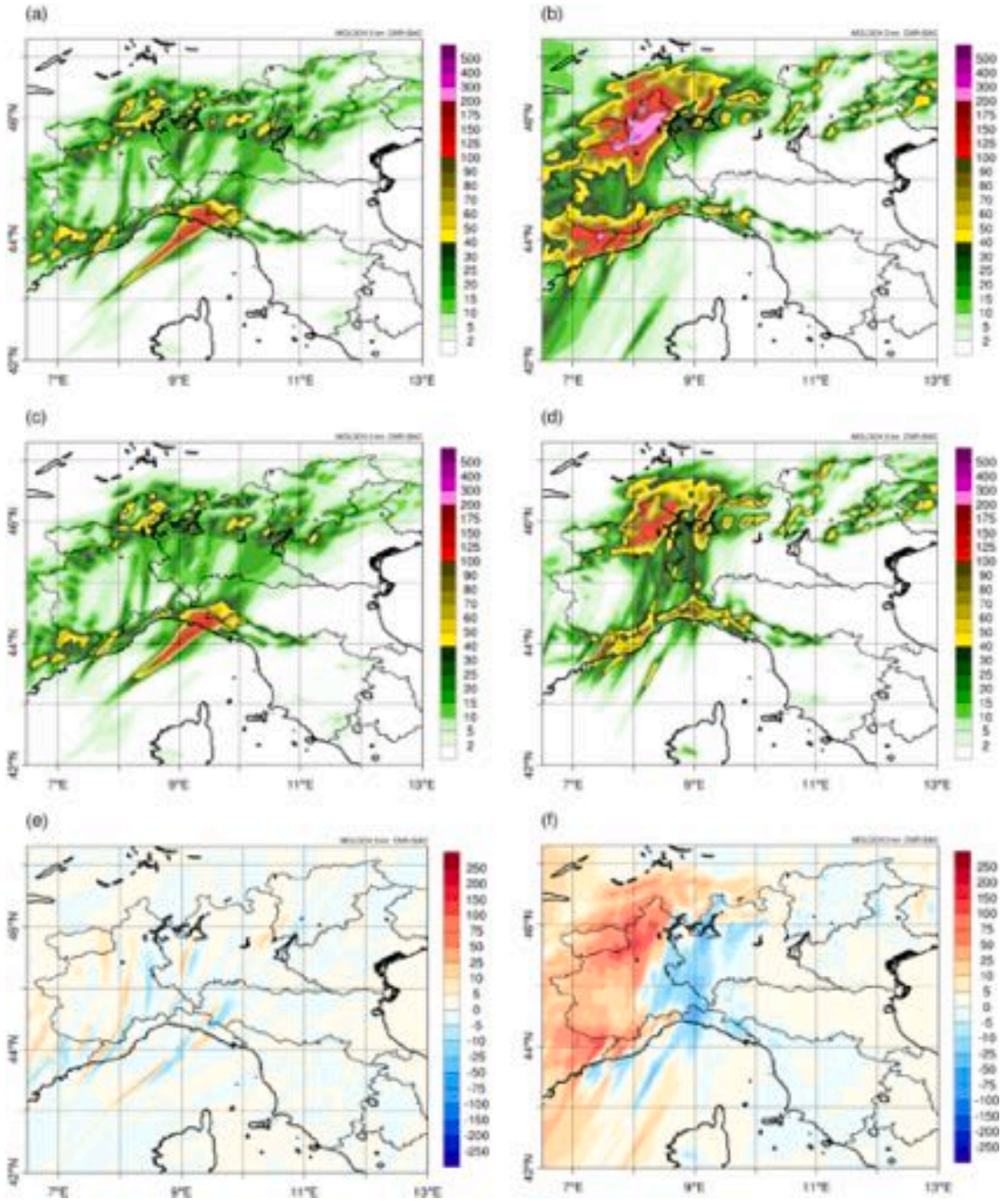

Fig. 15. The 12-h accumulated precipation simulated by MOLOCH in the first (a,c) and second (b, d) half of 2 October 2020. (a) and (b) refers to the CNTR simulation, while (c) and (d) are produced by the sensitivity experiment (see text). Difference of accumulated precipitation (e) and (f) between CNTR and sensitivity experiment in the two 12-h periods.

mesoscale characteristics, with other previous major floods, whose dynamical mechanisms were described by the conceptual model of heavy precipitation in the Alpine area proposed by Rotunno and Ferretti (2003). However, the novel and interesting aspect of this event consisted in the presence of an intense AR, suggested in a preliminary study of Magnusson et al. (2021), since this kind of moisture transport structures are not well studied in the Mediterranean yet. Therefore we sought to identify its role, and the results described the way it modified the previously known dynamical mechanisms of Alpine heavy precipitation, thus complementing the above-mentioned conceptual model.

Back-trajectory computations, an AR detection algorithm and high-resolution numerical simulations have allowed to investigate the large-scale moisture supply, the mesoscale dynamics and the inland moisture penetration through the Apennines and the Alps.

A primary finding of the present study is that heavy precipitation was critically supported by the AR, a narrow corridor of strong water vapour transport from the North Atlantic (even from the Gulf of Mexico) to the Mediterranean. Although it is known that moisture supply for heavy precipitation over northern Italy can come from the North Atlantic (e.g., Winschall et al., 2012) or in the form of AR from tropical Africa (e.g.,

Davolio et al., 2020a), we have shown that in this case the moisture supply was organized as an AR but coming from the North Atlantic.

The study focused mainly on lower-troposphere processes and akin to other infamous flood episodes in the area, this event shows the typical convergence and superposition of a colder (and stable) airflow coming from the east in the Po Valley that enhance the orographically forced uplift of a southerly moist and warm (moderately unstable) low-level jet over the Tyrrhenian Sea. It has been shown that in the present case the scene was made more complex due to the contribution of the AR within intense south-westerly currents which dominated in the middle troposphere, above 3000 m. The two southerly moist branches were thoroughly analysed and compared. While at the lower levels the combination of moisture content and wind speed produced a comparable intensity of water vapour transport, the component associated with the AR was characterized by a greater depth of relevant moisture flux, even above 5000 m.

The intensity of the AR has been evaluated and contextualized within the climatology of the period. This and the October 2018 event (Davolio et al., 2020a) share the ranking of extreme events, in terms of IVT, and they together disclose two possible different origins for ARs affecting the Mediterranean, and Italy in particular, respectively the Iberian Peninsula/Gibraltar Strait, and northern Africa. Further studies are needed to assess if other preferred regions for entrance exist, and also if the characteristics of the AR depend upon its region of origin. In fact, the October 2020 AR was thicker than that coming from the tropical Atlantic during the October 2018 event, since it was characterized by high values of moisture not confined in the lowest 3000 m, but extending even above 5000 m. This aspect can be relevant for detection techniques based on satellite WV channels. The comparison between the two events also revealed that, in spite of a similar intensity of moisture transport, different scenarios of heavy precipitation occur in response to the persistence and the geometrical characteristics of the AR.

Finally, the study has clearly shown that, in contrast with previous heavy rain events in the area, the slightly different synoptic features caused a much faster eastward evolution of the baroclinic wave, that did not amplify over the Mediterranean, thus limiting the persistence of the mesoscale pattern and of the precipitation. Therefore, in this case, the typical known mechanisms of intense Alpine rainfall would have not generated an extreme event since the precipitation system did not affect the same area long enough. In these conditions the AR contributed critically to the generation of heavy rainfall and turned the event into a devastating flood.

Given the relevance of ARs for heavy precipitation over the Alps, a detailed climatological analysis seems necessary. It will also allow to reveal if ARs were present in all the most intense rainfall episodes over northern Italy and how often they are associated with synoptic upper-troposphere disturbance affecting the Mediterranean.

cRediT author statement

Silvio Davolio: conceptualization, methodology, investigation, software, supervision, writing- original draft. **Marco Vercellino** and **Lucia Drago Pitura**: software, formal analysis and visualization. **Mario Marcello Miglietta**: conceptualization, methodology, investigation. Sante Laviola: investigation, visualization. **Vincenzo Levizzani**: conceptualization, supervision. All authors contributed to conceptualize the structure, organise the content of the article and reviewed the original draft.

Funding

This work has been supported by the Project “FOE-CLIMA Climate change: risk mitigation for sustainable development” funded by the Italian Ministry for Education, University and Research (MIUR).

Declaration of competing interest

The authors declare that they have no known competing financial interests or personal relationships that could have appeared to influence the work reported in this paper.

Data availability

Data will be made available on request.

Acknowledgments

The authors gratefully acknowledge (i) NOAA Air Resources Laboratory (ARL) for the provision of the HYSPLIT transport and dispersion model used in this publication; (ii) AEMET for providing the Palma sounding plots; (iii) The Italian Civil Protection Department for the data available through the DEWETRA interface.

References

ARPAL, 2020. Rapporto di evento meteo-idrologico dell’1-3 Ottobre 2020 (Report of the meteo-hydrological event of 1-3 October 2020). Accessed 23 January 2022. https://old.arpal.liguria.it/contenuti_statici//pubblicazioniodellii_eventi/2020/REM_20201001-03_Arancione_Rossa_vers20201112.pdf.

Bertò, A., Buzzi, A., Zardi, D., 2004. Back-tracking water vapour contributing to a precipitation event over Trentino: a case study. Meteor. Z. 13, 189–200. https://doi.org/10.1127/0941-2948/2004/0013-0189.

Bougeault, P., Binder, P., Buzzi, A., Dirks, R., Kuettner, J., Smith, R.B., Steinacker, R., Volkert, H., 2001. The MAP special observing period. Bull. Am. Meteorol. Soc. 82, 433–462. https://doi.org/10.1175/1520-0477(2001)082,0433:TMSOP. 2.3.CO;2.

Bozkurt, D., Ezber, Y., Sen, O.L., 2019. Role of the East Asian Trough on the eastern Mediterranean temperature variability in early spring and the extreme case of 2004 warm spell. Clim. Dynam. 53 (3–4), 2309–2326. https://doi.org/10.1007/s00382-019-04847-5.

Bruno, G., Pignone, F., Silvestro, F., Gabellani, S., Schiavi, F., Rebora, N., Giordano, P., Falzacappa, M., 2021. Performing hydrological monitoring at a national scale by exploiting rain-gauge and radar networks: the Italian case. Atmosphere 12, 771. https://doi.org/10.3390/atmos12060771.

Buzzi, A., Foschini, L., 2000. Mesoscale meteorological features associated with heavy precipitation in the Southern Alpine region. Meteorol. Atmos. Phys. 72, 131–146. https://doi.org/10.1007/s007030050011.

Buzzi, A., Davolio, S., Malguzzi, P., Drofa, O., Mastrangelo, D., 2014. Heavy rainfall episodes over Liguria of autumn 2011: numerical forecasting experiments. Nat. Hazards Earth Syst. Sci. 14, 1325–1340. https://doi.org/10.5194/nhess-14-1325-2014.

Buzzi, A., Di Muzio, E., Malguzzi, P., 2020. Barrier winds in the Italian region and effects of moist processes. Bull. Atmos. Sci. Technol. 1, 59–90. https://doi.org/10.1007/s42865-020-00005-6.

Cavaleri, L., Bajo, M., Barbariol, F., Bastianin, M., Benetazzo, A., Bertotti, L., Chiggiato, J., Davolio, S., Ferrarin, C., Magnusson, L., Papa, A., Pezzutto, P., Pomaro, A., Umgeisser, G., 2019. The October 29, 2018 storm in Northern Italy—an exceptional event and its modeling. Prog. Oceanogr. 178, 102178 https://doi.org/10.1016/j.pocean.2019.102178.

Chazette, P., Flamant, C., Shang, X., Totems, J., Raut, J.-C., Doerenbecher, A., Ducrocq, V., Fourrié, N., Bock, O., Cloché, S., 2016. A multi-instrument and multi-model assessment of atmospheric moisture variability over the western Mediterranean during HyMeX. Quart. J. Roy. Meteor. Soc. 142, 7–22. https://doi.org/10.1002/qj.2671.

Cremonini, R., Tiranti, D., 2018. The weather radar observations applied to shallow landslides prediction: a case study from North-Western Italy. Front. Earth Sci. 6, 134. https://doi.org/10.3389/feart.2018.00134.

Davolio, S., Della Fera, S., Laviola, S., Miglietta, M.M., Levizzani, V., 2020a. An atmospheric river in the Mediterranean basin: the 29 October 2018 “Vaia” storm over Italy. Mon. Weather Rev. 148, 3571–3588. https://doi.org/10.1175/MWR-D-20-0021.1.

Davolio, S., Malguzzi, P., Drofa, O., Mastrangelo, D., Buzzi, A., 2020b. The Piedmont flood of November 1994: a testbed of forecasting capabilities of the CNR-ISAC meteorological model suite. Bull. Atmos. Sci. Technol. 1, 263–282. https://doi.org/10.1007/s42865-020-00015-4.

Dayan, U., Nissen, K., Ulbrich, U., 2015. Review Article: atmospheric conditions inducing extreme precipitation over the eastern and western Mediterranean. Nat. Hazards Earth Syst. Sci. 15, 2525–2544. https://doi.org/10.5194/nhess-15-2525-2015.

de Vries, A.J., 2021. A global climatological perspective on the importance of Rossby wave breaking and intense moisture transport for extreme precipitation events. Weather Clim. Dynam. 2, 129–161. https://doi.org/10.5194/wcd-2-129-2021.

Drobinski, P., Ducrocq, V., Alpert, P., Anagnostou, E., Béranger, K., Borga, M., Braud, I., Chanzy, A., Davolio, S., Delrieu, G., Estournel, C., Filali Boubrahmi, N., Font, J., Grubisic, V., Gualdi, S., Homar, V., Ivančan-Picek, B., Kottmeier, C., Kotroni, V., Lagouvardos, K., Lionello, P., Llasat, M.C., Ludwig, W., Lutoff, C., Mariotti, A., Richard, E., Romero, R., Rotunno, R., Roussot, O., Ruin, I., Somot, S., Taupier-

Letage, I., Tintore, J., Uijlenhoet, R., Wernli, H., 2014. HyMeX, a 10-year multidisciplinary program on the Mediterranean water cycle. Bull. Am. Meteorol. Soc. 95, 1063–1082. https://doi.org/10.1175/BAMS-D-12-00242.1.

Ducrocq, V., Braud, I., Davolio, S., Ferretti, R., Flamant, C., Jansa, A., Kalthoff, N., Richard, E., Taupier-Letage, I., Ayral, P.-A., Belamari, S., Berne, A., Borga, M., Boudevillain, B., Bock, O., Boichard, J.-L., Bouin, M.-N., Bousquet, O., Bouvier, C., Chiggiato, J., Cimini, D., Corsmeier, U., Coppola, L., Cocquerez, P., Defer, E., Drobinski, P., Dufournet, Y., Fourrié, N., Gourley, J.J., Labatut, L., Lambert, D., Le Coz, J., Marzano, F.S., Molinié, G., Montani, A., Nord, G., Nuret, M., Ramage, K., Rison, B., Roussot, O., Said, F., Schwarzenboeck, A., Testor, P., Van Baelen, J., Vincendon, B., Aran, M., Tamayo, J., 2014. HyMeX SOP1, the field campaign dedicated to heavy precipitation and flash flooding in the northwestern Mediterranean. Bull. Am. Meteorol. Soc. 95, 1083–1100. https://doi.org/10.1175/BAMS-D-12-00244.1.

Eiras-Barca, J., Ramos, A.M., Algarra, I., Vázquez, M., Dominguez, F., Miguez-Macjho, G., Nieto, R., Gimeno, L., Taboada, J., Ralph, F.M., 2021. European West Coast atmospheric rivers: a scale to characterize strength and impacts. Weather Clim. Extrem. 31, 100305 https://doi.org/10.1016/j.wace.2021.100305.

Francis, D., Fonseca, R., Nelli, N., Bozkurt, D., Picard, G., Guan, B., 2022. Atmospheric rivers drive exceptional Saharan dust transport towards Europe. Atmos. Res. 266, 105959. https://doi.org/10.1016/j.atmosres.2021.105959.

Giovannini, L., Davolio, S., Zaramella, M., Zardi, D., Borga, M., 2021. Multi-model convection-resolving simulations of the October 2018 Vaia storm over Northeastern Italy. Atmos. Res. 253, 1–20. https://doi.org/10.1016/j.atmosres.2021.105455.

Grazzini, F., Craig, G.C., Keil, C., Antolini, G., Pavan, V., 2020a. Extreme precipitation events over northern Italy. Part I: a systematic classification with machine-learning techniques. Quart. J. Roy. Meteor. Soc. 146, 69–85. https://doi.org/10.1002/qj.3635.

Grazzini, F., Fragkoulidis, G., Pavan, V., Antolini, G., 2020b. The 1994 Piedmont flood: an archetype of extreme precipitation events in Northern Italy. Bull. Atmos. Sci. Technol. 1, 283–295. https://doi.org/10.1007/s42865-020-00018-1.

Grazzini, F., Fragkoulidis, G., Teubler, F., Wirth, V., Craig, G.C., 2021. Extreme precipitation events over northern Italy. Part II: dynamical precursors. Quart. J. Roy. Meteor. Soc. 147, 1237–1257. https://doi.org/10.1002/qj.3969.

Guan, B., Waliser, D.E., 2015. Detection of atmospheric rivers—evaluation and application of an algorithm for global studies. J. Geophys. Res. Atmos. 120, 12514–12535. https://doi.org/10.1002/2015JD0245257.

Hersbach, H., Bell, B., Berrisford, P., Hirahara, S., Horányi, A., Muñoz-Sabater, J., Nicolas, J., Peubey, C., Radu, R., Schepers, D., Simmons, A., Soci, C., Abdalla, S., Abellan, X., Balsamo, G., Bechtold, P., Biavati, G., Bidlot, J., Bonavita, M., De Chiara, G., Dahlgren, P., Dee, D., Diamantakis, M., Dragani, R., Flemming, J., Forbes, R., Fuentes, M., Geer, A., Haimberger, L., Healy, S., Hogan, R.J., Hólm, E., Janisková, M., Keeley, S., Laloyaux, P., Lopez, P., Lupu, C., Radnoti, G., de Rosnay, P., Rozum, I., Vamborg, F., Villaume, S., Thépaut, J.-N., 2020. The ERA5 global reanalysis. Quart. J. Roy. Meteor. Soc. 146, 1999–2049. https://doi.org/10.1002/qj.3803.

Hubbard, M.E., Nikiforakis, N., 2003. A three-dimensional adaptive, Godunov type model for global atmospheric flows I: tracer advection on fixed grids. Mon. Weather Rev. 131, 1848–1864. https://doi.org/10.1175//2568.1.

Isotta, F.A., Frei, C., Weilguni, V., Perčec Tadić, M., Lassègues, P., Rudolf, B., Pavan, V., Cacciamani, C., Antolini, G., Ratto, S.M., Munari, M., Micheletti, S., Bonati, V., Lussana, C., Ronchi, C., Panettieri, E., Marigo, G., Vertačnik, G., 2014. The climate of daily precipitation in the Alps: development and analysis of a high-resolution grid dataset from pan-Alpine rain-gauge data. Int. J. Climatol. 34, 1657–1675. https://doi.org/10.1002/joc.3794.

Italian Civil Protection Department, CIMA Research Foundation, 2014. The Dewetra platform: a multi-perspective architecture for risk management during emergencies. In: Hanachi, C., Bénaben, F., Charoy, F. (Eds.), Information Systems for Crisis Response and Management in Mediterranean Countries. ISCRAM-med 2014. Lecture Notes in Business Information Processing, 196. Springer, Cham, Switzerland, pp. 165–177.

Kain, J.S., 2004. The Kain–Fritsch convective parameterization: an update. J. Appl. Meteorol. 43, 170–181. https://doi.org/10.1175/1520-0450(2004)043<0170:TKCPAU>2.0.CO;2.

Khodayar, S., Czajka, B., Caldas-Alvarez, A., Helgert, S., Flamant, C., Di Girolamo, P., Bock, O., Chazette, P., 2018. Multi-scale observations of moisture feeding heavy precipitating systems in the north-western Mediterranean during HyMeX IOP12. Quart. J. Roy. Meteor. Soc. 144, 2761–2780. https://doi.org/10.1002/qj.3402.

Khodayar, S., Davolio, S., Di Girolamo, P., Lebeaupin Brossier, C., Flaounas, E., Fourrie, N., Lee, K.-O., Ricard, D., Vie, B., Bouttier, F., Caldas-Alvarez, A., Ducrocq, V., 2021. Overview towards improved understanding of the mechanisms leading to heavy precipitation in the western Mediterranean: lessons learned from HyMeX. Atmos. Chem. Phys. 21, 17051–17078. https://doi.org/10.5194/acp-21-17051-2021.

Krichak, S.O., Barkan, J., Breitgand, J.S., Gualdi, S., Feldstein, S.B., 2015. The role of the export of tropical moisture into midlatitudes for extreme precipitation events in the Mediterranean region. Theor. Appl. Climatol. 121, 499–515. https://doi.org/10.1007/s00704-014-1244-6.

Lorente-Plazas, R., Montavez, J.P., Ramos, A.M., Jerez, S., Trigo, R.M., Jimenez-Guerrero, P., 2019. Unusual atmospheric-river-like structures coming from Africa induced extreme precipitation over the western Mediterranean Sea. J. Geophys. Res. Atmos. 125, e2019JD031280 https://doi.org/10.1029/2019JD031280.

Magnusson, L., Hewson, T., Lavers, D., 2021. Windstorm Alex affected large parts of Europe. ECMWF Newsletter 166, 4–5 [available at. https://www.ecmwf.int/en/newsletter/166/news/windstorm-alex-affected-large-parts-europe].

Mahovic, N.S., Nietosvaara, V., 2020. Europe was battered during the first October weekend in 2020, with extensive storms, extreme rainfall and flooding. Available at last accessed 04 November. 2022. https://www.eumetsat.int/storms-hit-france-early-october.

Malguzzi, P., Grossi, G., Buzzi, A., Ranzi, R., Buizza, R., 2006. The 1966 'century' flood in Italy: a meteorological and hydrological revisitation. J. Geophys. Res. 111, D24106 https://doi.org/10.1029/2006JD007111.

Massacand, A.C., Wernli, H., Davies, H.C., 1998. Heavy precipitation on the Alpine southside: an upper-level precursor. Geophys. Res. Lett. 25, 1435–1438. https://doi.org/10.1029/98GL50869.

Miglietta, M.M., Davolio, S., 2022. Dynamical forcings in heavy precipitation events over Italy: lessons from the HyMeX SOP1 campaign. Hydrol. Earth Syst. Sci. 26, 627–646. https://doi.org/10.5194/hess-26-627-2022.

Miglietta, M.M., Rotunno, R., 2014. Numerical simulations of sheared conditionally unstable flows over a mountain ridge. J. Atmos. Sci. 71, 1747–1762. https://doi.org/10.1175/JAS-D-13-0297.1.

Milelli, M., Llasat, M.C., Ducroq, V., 2006. The cases of June 2000, November 2002 and September 2002 as examples of Mediterranean floods. Nat. Hazards Earth Syst. Sci. 6, 271–284. https://doi.org/10.5194/nhess-6-271-2006.

Morcrette, J.J., Barker, H.W., Cole, J.N.S., Iacono, M.J., Pincus, R., 2008. Impact of a new radiation package, McRad, in the ECMWF integrated forecasting system. Mon. Weather Rev. 136, 4773–4798. https://doi.org/10.1175/2008 MWR2363.1.

Mueller, M.J., Mahoney, K.M., Hughes, M., 2017. High-resolution model-based investigation of moisture transport into the Pacific Northwest during a strong atmospheric river event. Mon. Weather Rev. 145, 3861–3879. https://doi.org/10.1175/MWR-D-16-0466.1.

Piemonte, A.R.P.A., 2020. Evento del 2-3 Ottobre 2020 (2-3 October 2020 event). Accessed 23 January 2022. http://www.arpa.piemonte.it/pubblicazioni-2/relazioni-tecniche/analisi-eventi/eventi-2020/2020-rapporto-evento-02-ottobre.pdf.

Pinto, J.G., Ulbrich, S., Parodi, A., Rudari, R., Boni, G., Ulbrich, U., 2013. Identification and ranking of extraordinary rainfall events over Northwest Italy: the role of Atlantic moisture. J. Geophys. Res. Atmos. 118, 2085–2097. https://doi.org/10.1002/JGRD.50179.

Ralph, F.M., Dettinger, M.D., Cairns, M.M., Galarneau, T.J., Eylander, J., 2018. Defining "atmospheric river'': how the Glossary of Meteorology helped resolve a debate. Bull. Am. Meteorol. Soc. 99, 837–839. https://doi.org/10.1175/BAMS-D- 17-0157.1.

Ralph, F.M., Rutz, J.J., Cordeira, J.M., Dettinger, M., Anderson, M., Reynolds, D., Schick, L.J., Smallcomb, C., 2019. A scale to characterize the strength and impacts of atmospheric rivers. Bull. Amer. Meteor. 100, 269–289.

Ritter, B., Geleyn, J.F., 1992. A comprehensive radiation scheme for numerical weather prediction models with potential applications in climate simulations. Mon. Weather Rev. 120, 303–325. https://doi.org/10.1175/1520- 0493(1992)120<0303:ACRSFN>2.0.CO;2.

Rolph, G., Stein, A., Stunder, B., 2017. Real-time environmental applications and display sYstem: READY. Environ. Model. Software 95, 210–228. https://doi.org/10.1016/j.envsoft.2017.06.025.

Rotunno, R., Ferretti, R., 2001. Mechanisms of intense Alpine rainfall. J. Atmos. Sci. 58, 1732–1749. https://doi.org/10.1175/1520-0469(2001)058<1732:MOIAR>2.0.CO;2.

Rotunno, R., Ferretti, R., 2003. Orographic effects on rainfall in MAP cases IOP2b and IOP8. Quart. J. Roy. Meteor. Soc. 129, 373–390. https://doi.org/10.1256/qj.02.20.

Rotunno, R., Houze, R.A., 2007. Lessons on orographic precipitation from the mesoscale Alpine Programme. Quart. J. Roy. Meteor. Soc. 133, 811–830. https://doi.org/10.1002/qj.67.

Sanders, F., Gyakum, J.R., 1980. Synoptic-dynamic climatology of the "bomb. Mon. Weather Rev. 108, 1589–1606. https://doi.org/10.1175/1520-0493(1980)108,1589:SDCOT.2.0.CO;2.

Smith, R.B., Jiang, Q., Fearon, M.G., Tabary, P., Dorninger, M., Doyle, J.D., Beniot, R., 2003. Orographic precipitation and air masses transformat ion: an Alpine example. Quart. J. Roy. Meteor. Soc. 129, 433–454.

Smith, B.L., Yuter, S.E., Neiman, P.J., Kingsmill, D.E., 2010. Water vapor fluxes and orographic precipitation over North California associated with a landfalling atmospheric river. Mon. Weather Rev. 138, 74–100. https://doi.org/10.1175/2009MWR2939.1.

Sodemann, H., Zubler, E., 2010. Seasonal and inter-annual variability of the moisture sources for Alpine precipitation during 1995-2002. Int. J. Climatol. 30 (7), 947–961. https://doi.org/10.1002/joc.1932.

Stein, A.F., Draxler, R.R., Rolph, G.D., Stunder, B.J.B., Cohen, M.D., Ngan, F., 2015. NOAA's HYSPLIT atmospheric transport and dispersion modeling system. Bull. Am. Meteorol. Soc. 96, 2059–2077. https://doi.org/10.1175/BAMS-D-14-00110.1.

Trini Castelli, S., Bisignano, A., Donateo, A., Landi, T.C., Martano, P., Malguzzi, P., 2020. Evaluation of the turbulence parametrization in the MOLOCH meteorological model. Quart. J. Roy. Meteor. Soc. 146, 124–140. https://doi.org/10.1002/qj.3661.

Turato, B., Reale, O., Siccardi, F., 2004. Water vapor sources of the October 2000 Piedmont flood. J. Hydrometeorol. 5, 693–712. https://doi.org/10.1175/1525-7541(2004)005,0693: WVSOTO.2.0.CO;2.

Winschall, A., Pfahl, S., Sodemann, H., Wernli, H., 2012. Impact of North Atlantic evaporation hot spots on southern Alpine heavy precipitation events. Quart. J. Roy. Meteor. Soc. 138, 1245–1258. https://doi.org/10.1002/qj.987.

Winschall, A., Sodemann, H., Pfahl, S., Wernli, H., 2014. How important is intensified evaporation for Mediterranean precipitation extremes? J. Geophys. Res. Atmos. 119, 5240–5256. https://doi.org/10.1002/2013JD021175.

Zampieri, M., Malguzzi, P., Buzzi, A., 2005. Sensitivity of quantitative precipitation forecasts to boundary layer parameterization: a flash flood case study in the western Mediterranean. Nat. Hazards Earth Syst. Sci. 5, 603–612. https://doi.org/10.5194/nhess-5-603-2005.